FLUX ROPES, TURBULENCE, AND COLLISIONLESS PERPENDICULAR SHOCK WAVES: HIGH PLASMA BETA CASE[1]

G.P. Zank, M. Nakanotani, L.-L. Zhao, S. Du, & L. Adhikari

Department of Space Science and Center for Space Plasma and Aeronomic Research
University of Alabama in Huntsville

[1]Zank et al., 2021, submitted

OUTLINE:

1) **Motivation & Background:** the transmission of fluctuations through boundaries and discontinuities

2) **How does turbulence interact with shocks?** Idealized theory and results

3) **Comparison of (idealized) theory with heliospheric observations:** Applicability of idealized theory for events at 1, 5, and 84 au, magnetic, kinetic energy, and density variance spectra

4) **Concluding remarks**

5) **Some final thoughts about the evolution of turbulence behind a shock:** simulations

1) **Why the transmission of fluctuations through boundaries and discontinuities is interesting aka Motivation & Background**

MOTIVATION 1)

Burlaga et al. (2015, 2018)

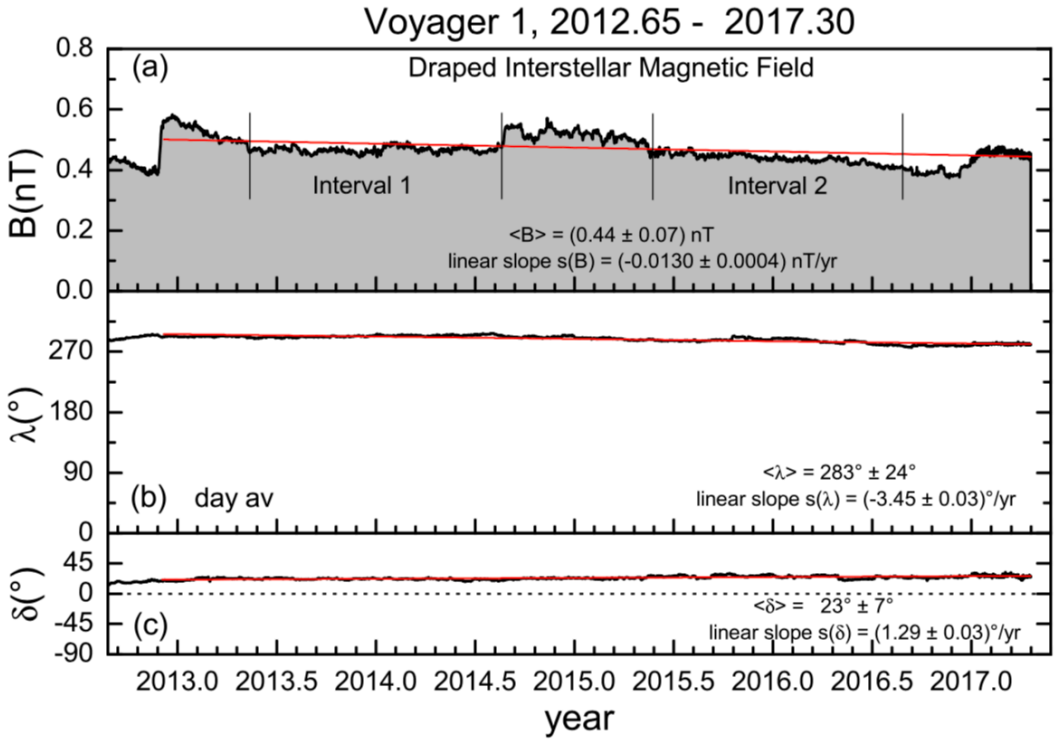

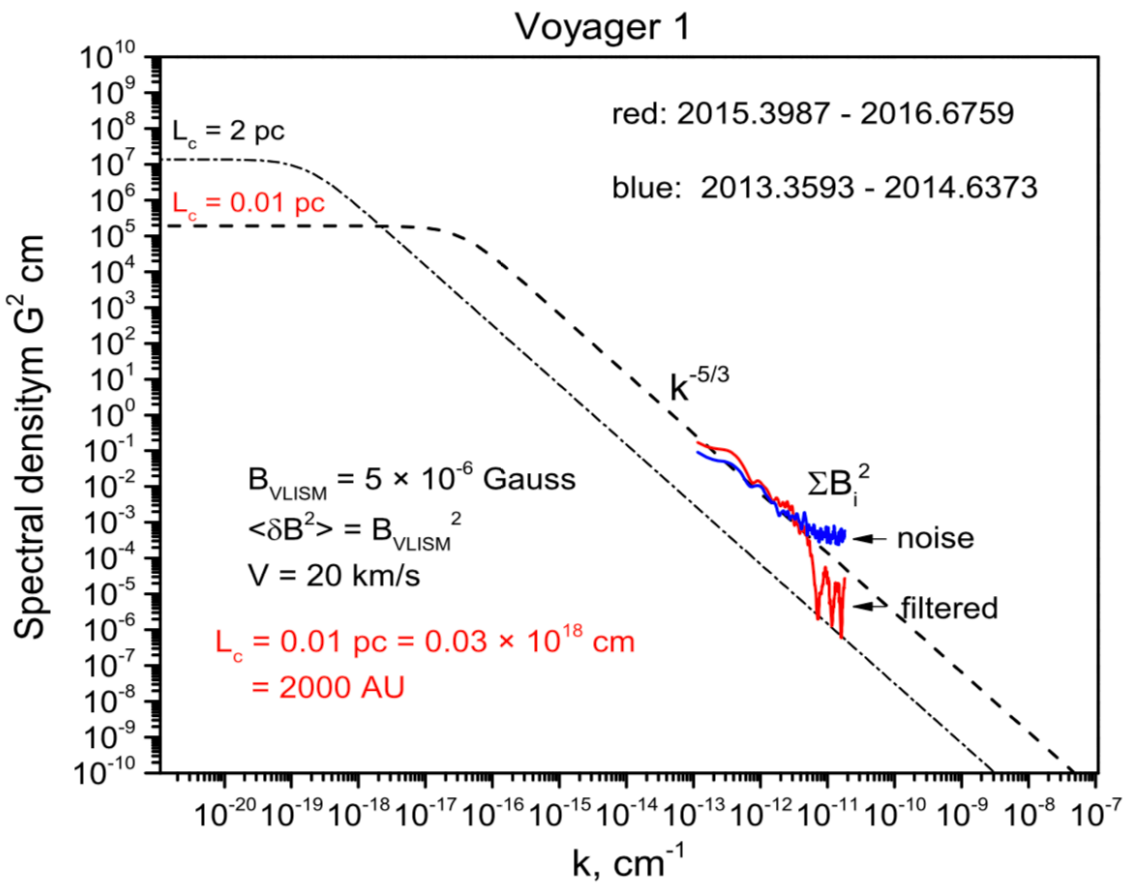

Interval 1: Compressible turbulence with the fluctuating magnetic field almost entirely parallel to VLISM mean magnetic field, and exhibiting ~$k^{-5/3}$ spectrum in $dB_{||}$

Interval 2: Incompressible turbulence almost exclusively, exhibiting ~$k^{-5/3}$ spectrum in $dB_{\perp}$ with same amplitude as $dB_{||}$

These surprising observations raise three important questions:

i) What is the ***origin of the compressible fluctuations in the VLISM***? and

ii) is the observed magnetic turbulence spectrum representative of interstellar turbulence in a partially ionized interstellar plasma, or is it somehow another manifestation of the mediation of the VLISM by heliospheric processes?

iii) Since fast magnetosonic waves can propagate further into the VLISM, why are these modes not seen in Interval 2?

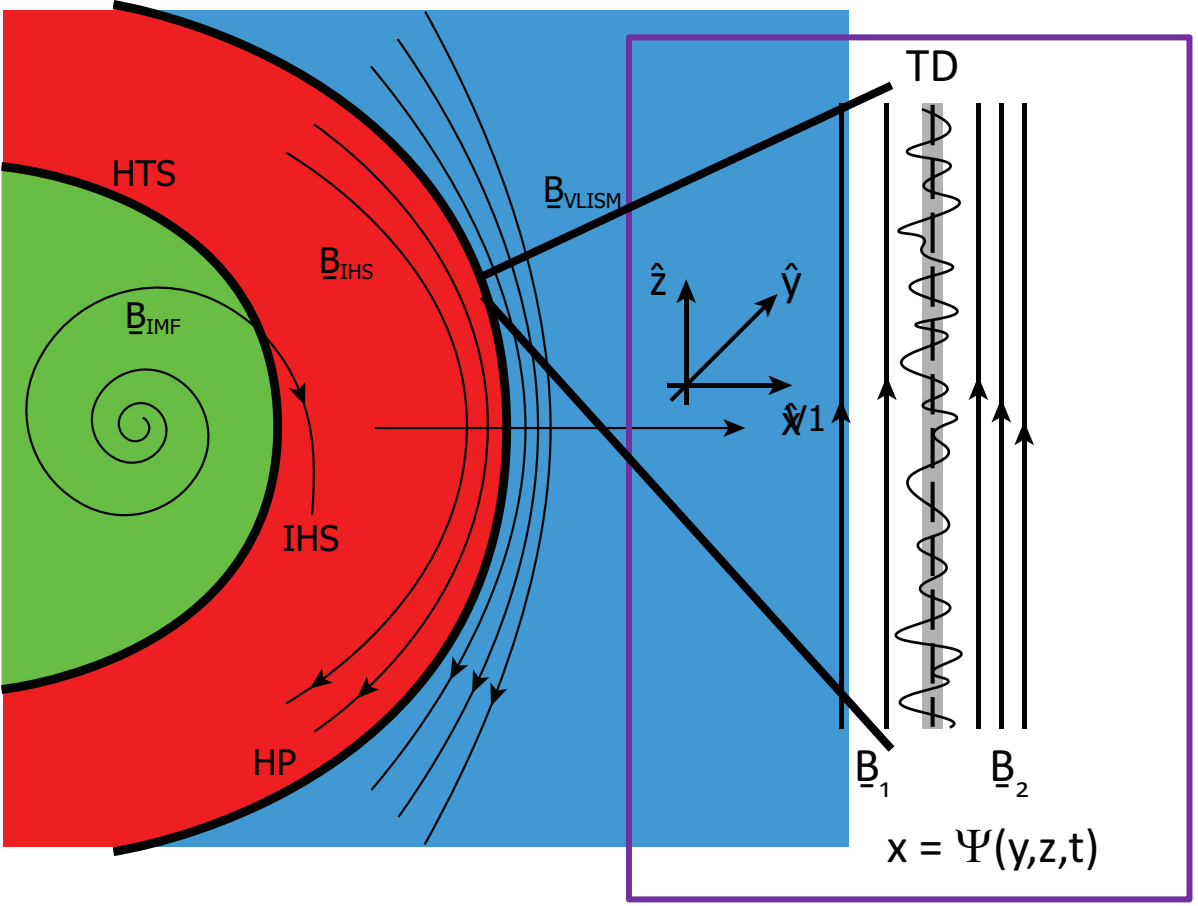

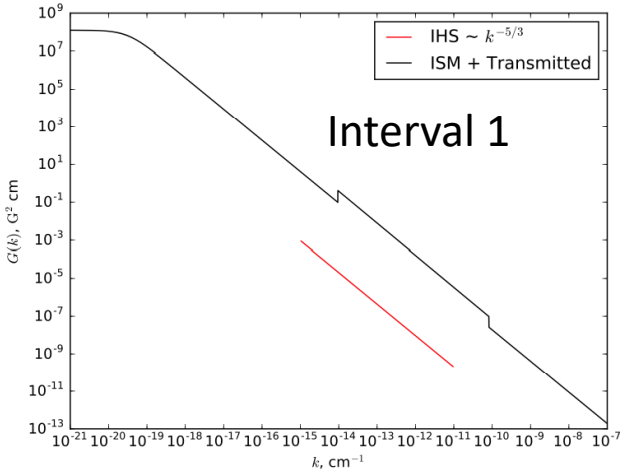

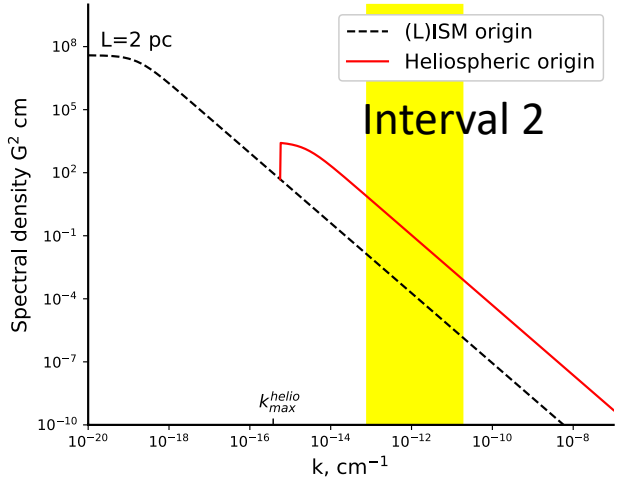

Figure 8. Illustration of the expected form of the VLISM power spectral density for magnetic field fluctuations. A background interstellar spectrum of the form $G(k) = (5\sin(3\pi/5)/6\pi)\ [\langle\delta\hat{B}^2\rangle L/(1+(kL)^{5/3})]$ (Giacalone & Jokipii 1999; Zank 2014) is assumed, and $L = 10$ pc [illegible] et al. 2015), to which is added the transmitted fas[illegible] Figure 6. As before, the HP parameters are $\gamma = 5/$[illegible] and $r = 100$.

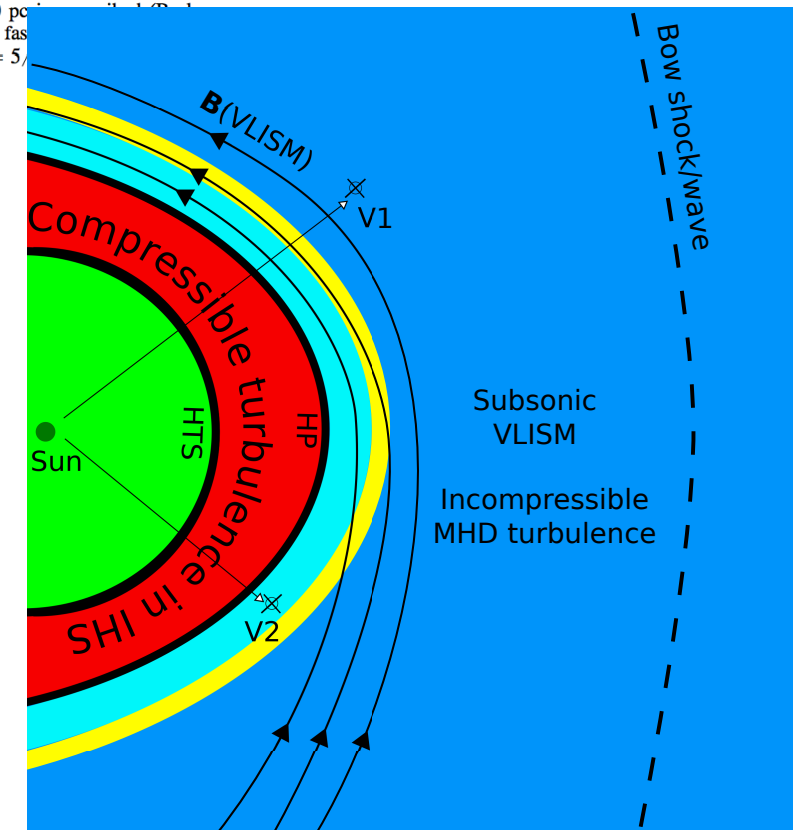

- ***IHS fast- and slow-mode waves incident on the HP generate only highly oblique fast-mode waves that propagate into the VLISM.***
- VLISM fast-mode waves contribute magnetic fluctuations b_{z2} \neq 0 parallel to the VLISM magnetic field and do not enhance the power in transverse modes
- ***Fast magnetosonic waves undergo mode conversion via three-wave interaction*** as they propagate in the homogeneous VLISM, ***decaying into an Alfvén wave and a zero-frequency Elsässer vortex***, both of which possess only a transverse magnetic field component $dB_{\perp}$. (Zank et al 2017, 2019)

k// and k⊥ are the ingredients of Slab and 2D turbulence model

SOME BACKGROUND: MAGNETIC FLUX ROPES *AKA* MAGNETIC ISLANDS

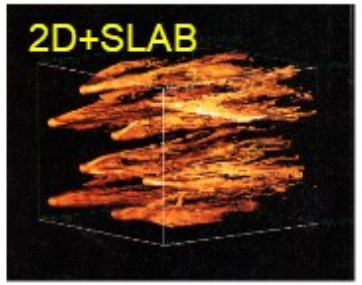

[Bieber et al., 1996]

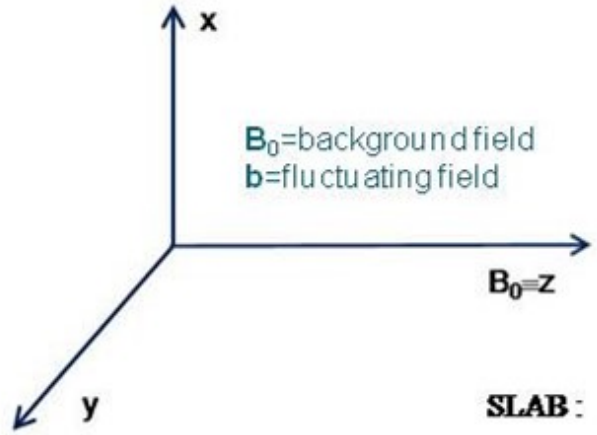

$$e^{-i(\omega t-\vec{k}\cdot\vec{r})} \Rightarrow k_x \sim \frac{\partial}{\partial x}; k_y \sim \frac{\partial}{\partial y}; k_z \sim \frac{\partial}{\partial z}$$

$$\textbf{SLAB}: \quad b \equiv \left(b_x(z), b_y(z), 0\right) \Rightarrow \frac{\partial}{\partial x} = \frac{\partial}{\partial y} = 0 \Rightarrow k_x = k_y = 0 \Rightarrow k \equiv (0,0,k_z) \Rightarrow k_{//}$$

$$\textbf{2-D}: \quad b \equiv \left(b_x(x,y), b_y(x,y), 0\right) \Rightarrow \frac{\partial}{\partial x} \neq 0; \frac{\partial}{\partial y} \neq 0; \frac{\partial}{\partial z} = 0 \Rightarrow k \equiv (k_x, k_y, 0) \Rightarrow k_{\perp}$$

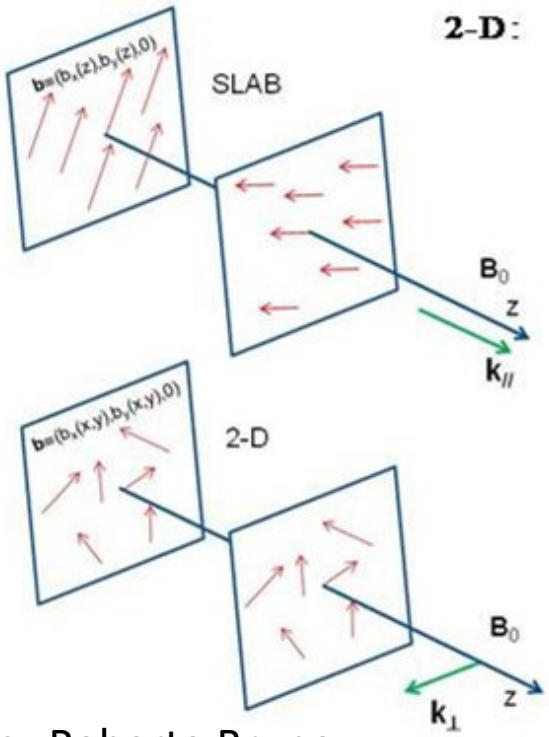

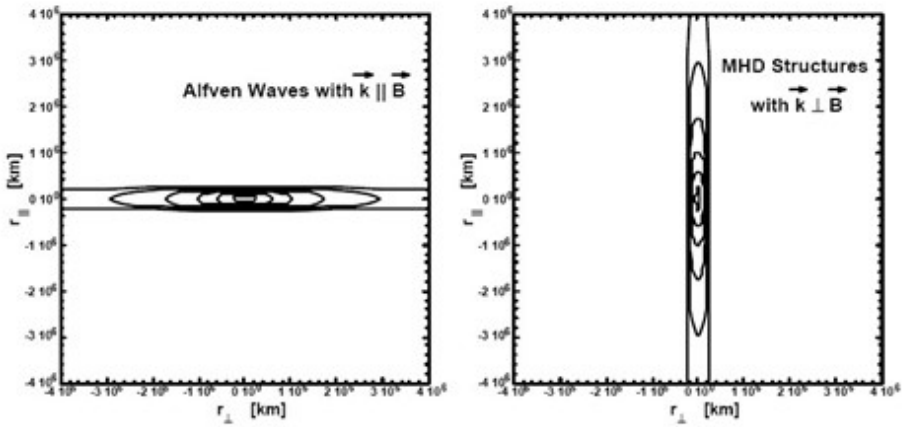

[Bieber et al., 1996]

❑ Axisimmetry assumed

Courtesy Roberto Bruno

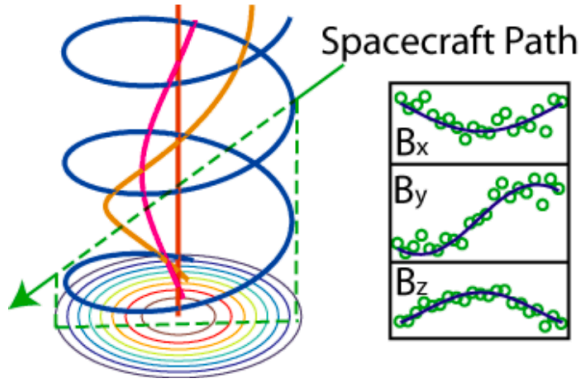

Magnetic flux rope structure

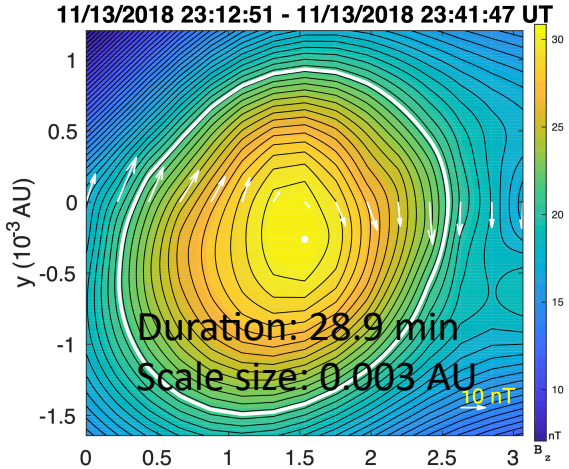

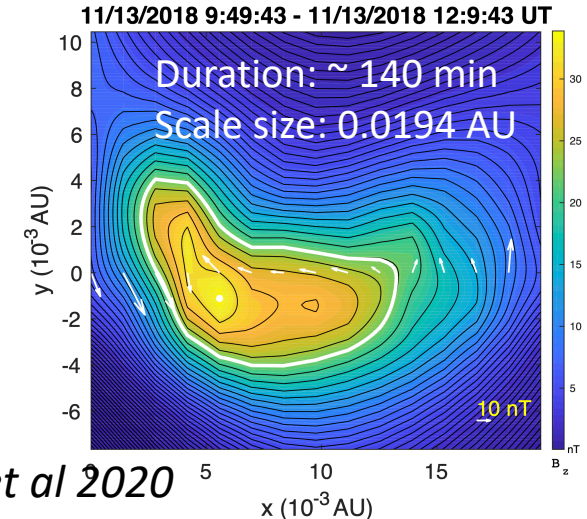

Zhao et al 2020

Motivation 2): Ulysses observations near 5 AU

Zhao et al. 2018, 2019a. *ApJ*

Flux enhancement downstream of the shock

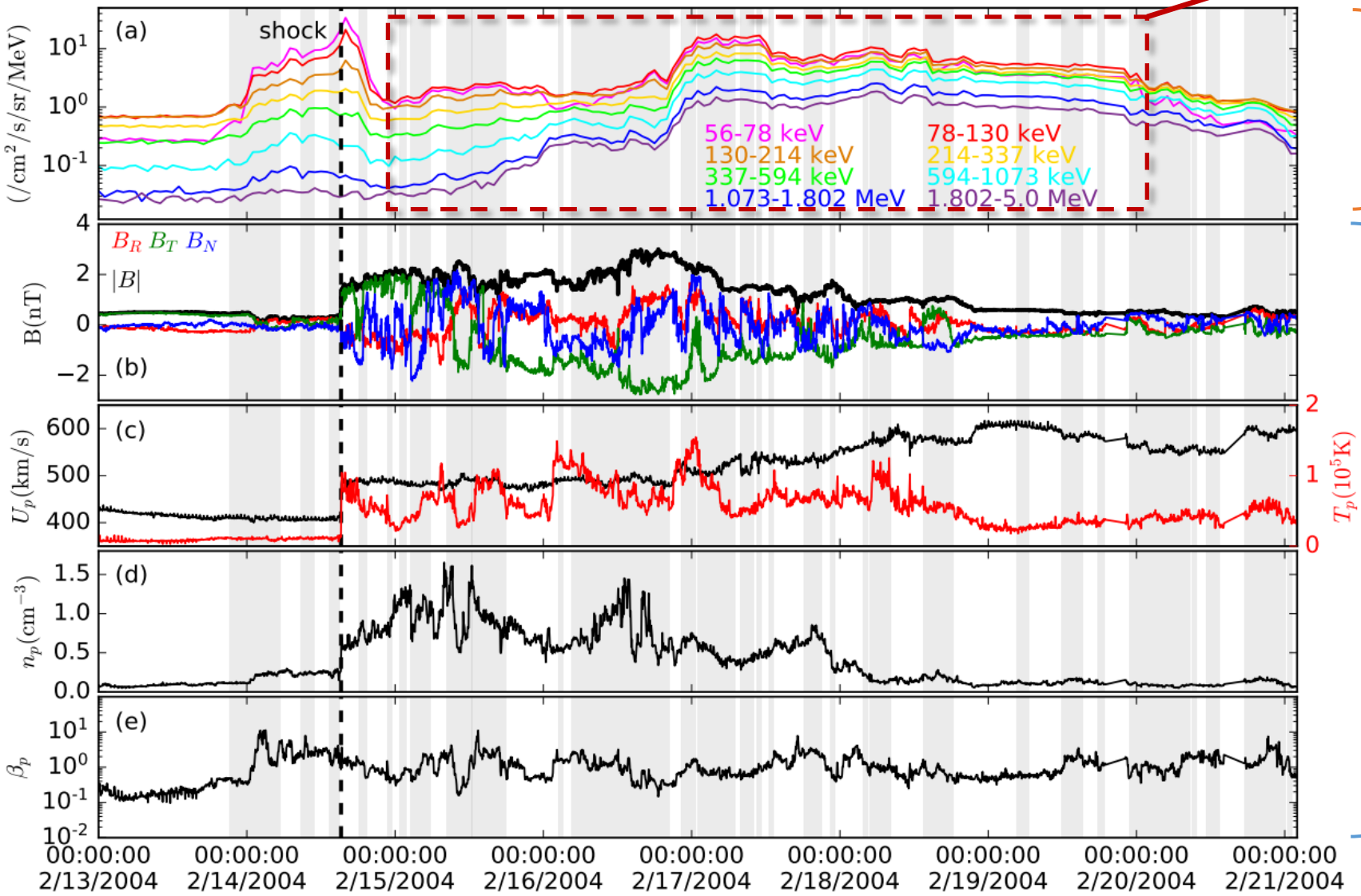

Energetic proton flux measured by *Ulysses* LEMS30

Magnetic field and plasma parameters: (b) **magnetic field** components and magnitude, (c) proton **speed and temperature**, (d) proton number **density**, and (e) **proton beta**.

- During this period, Ulysses crossed the **heliographic equator at 5.36 AU**.
- A fast forward shock was detected at 15:15:27 UT on 02/14/2004.

We automatically identify 31 **magnetic flux rope structures (grey shaded areas).**

Particle acceleration & SMFR

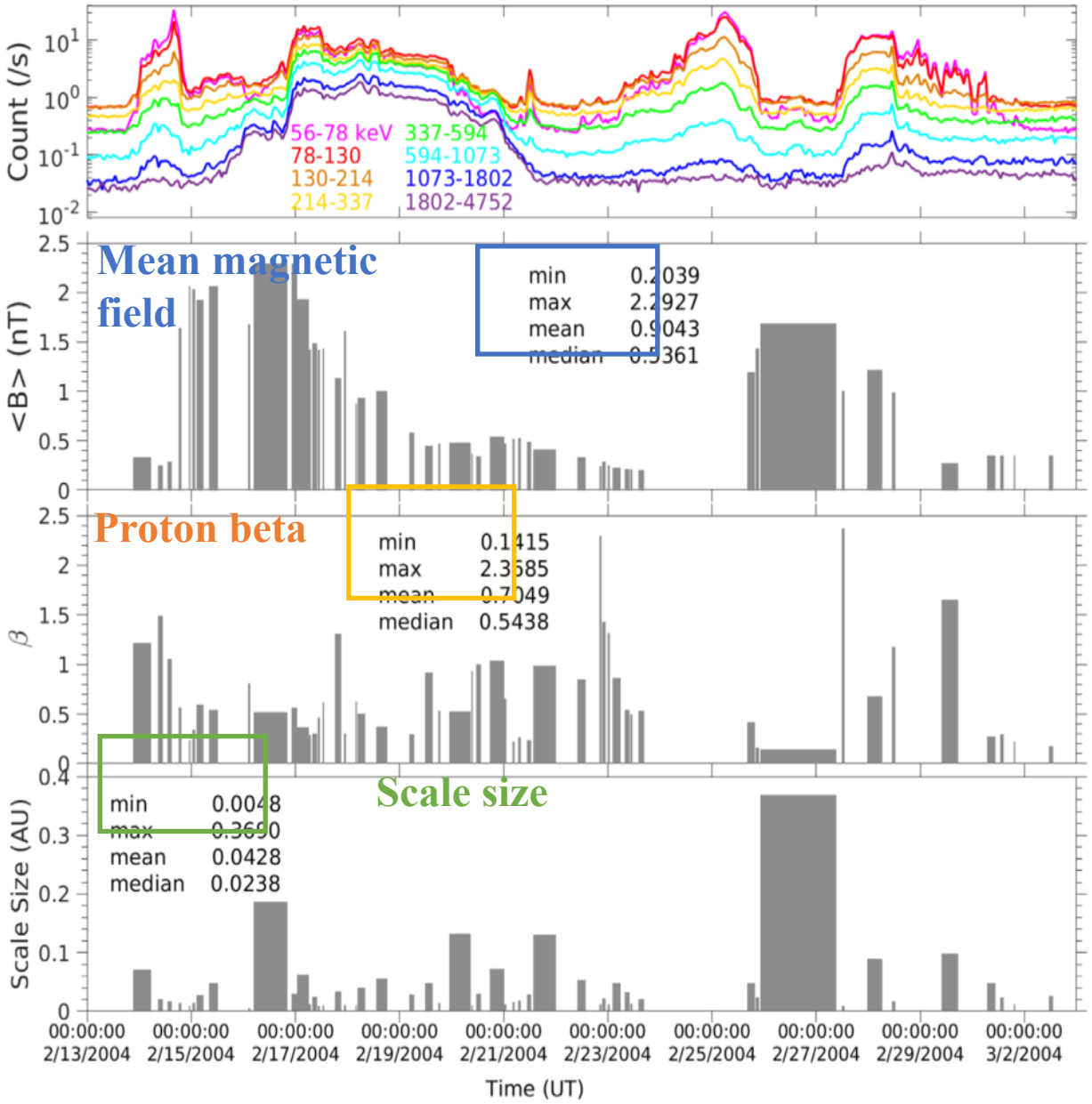

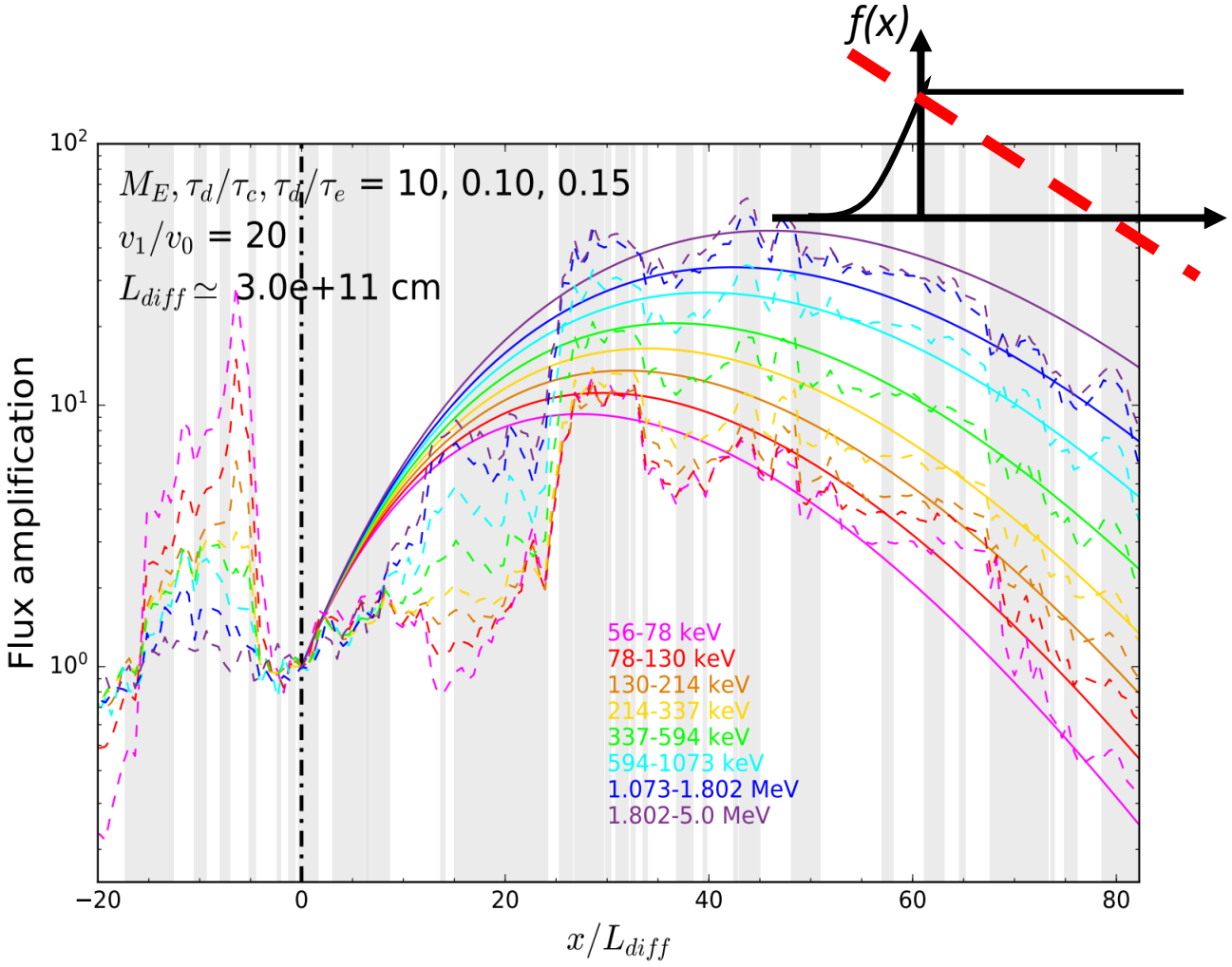

Stochastic acceleration by interacting magnetic islands accounts successfully for the observed energetic proton flux amplification (Zank et al. 2014, 2015; Zhao et al. 2018, 2019a).

Voyager 2 observation

Zhao et al. 2019b. *ApJ*

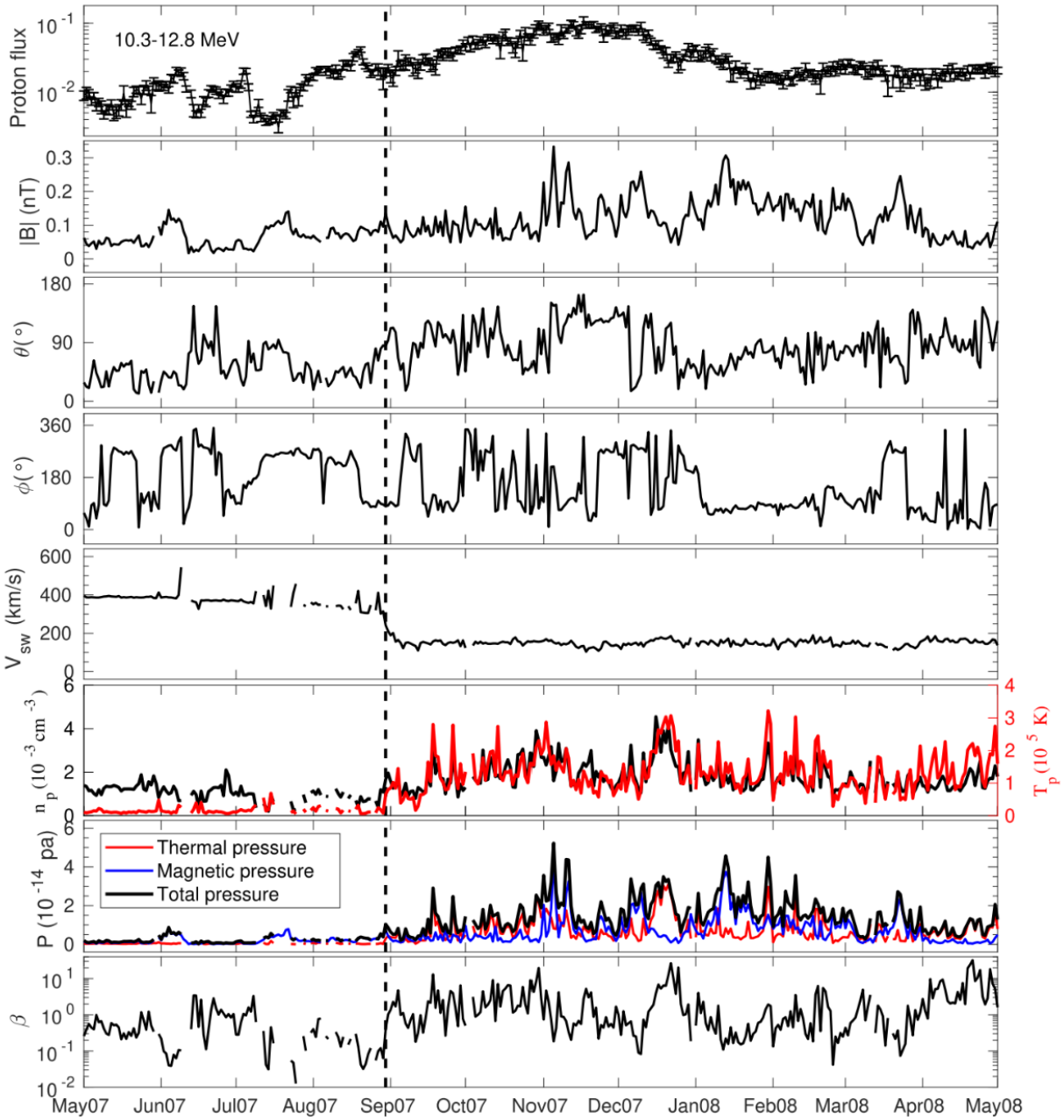

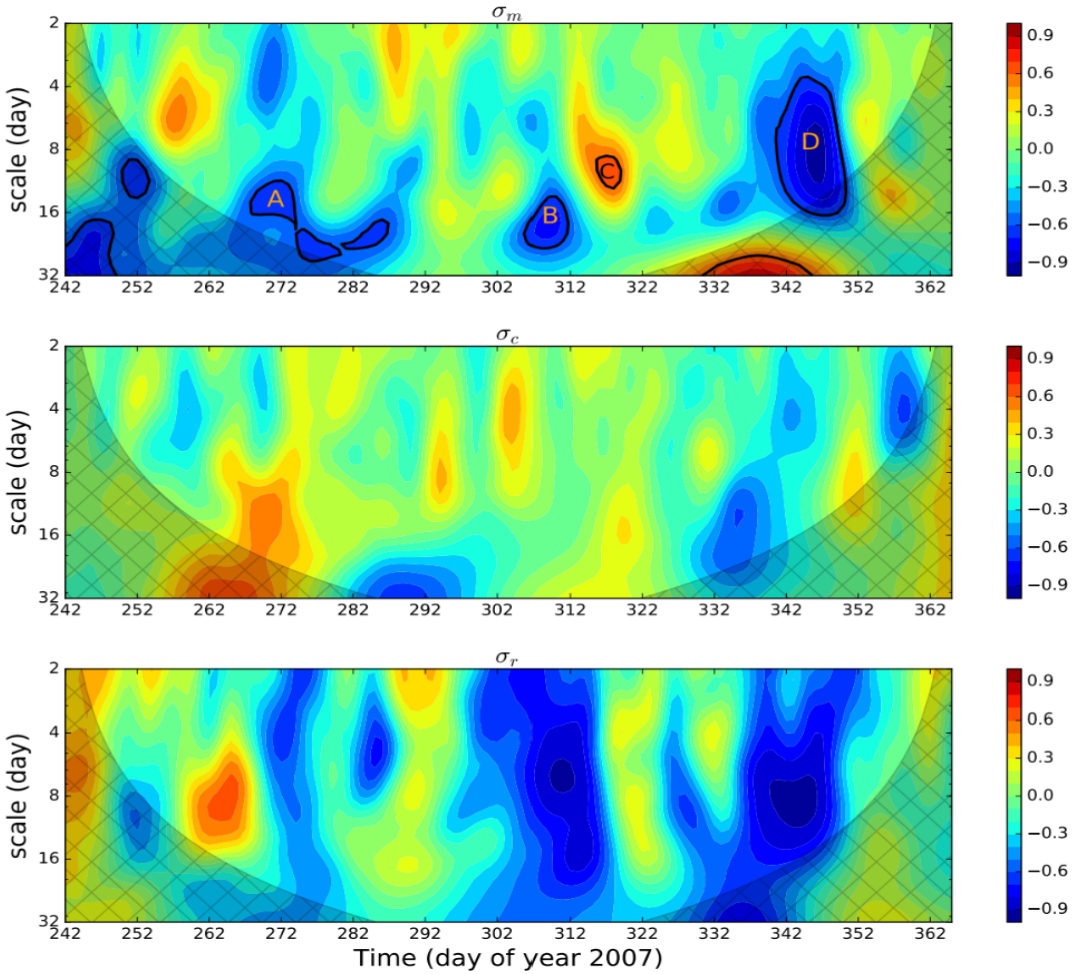

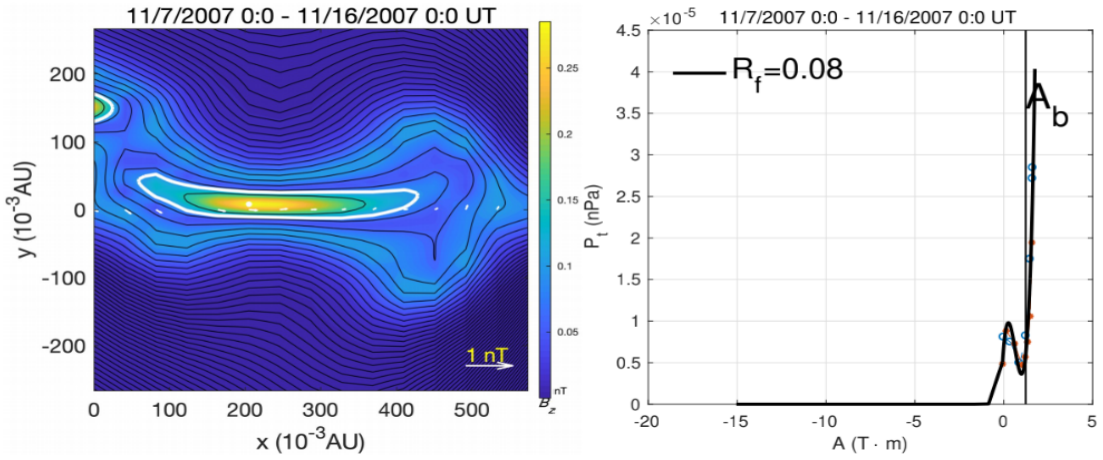

ACR acceleration

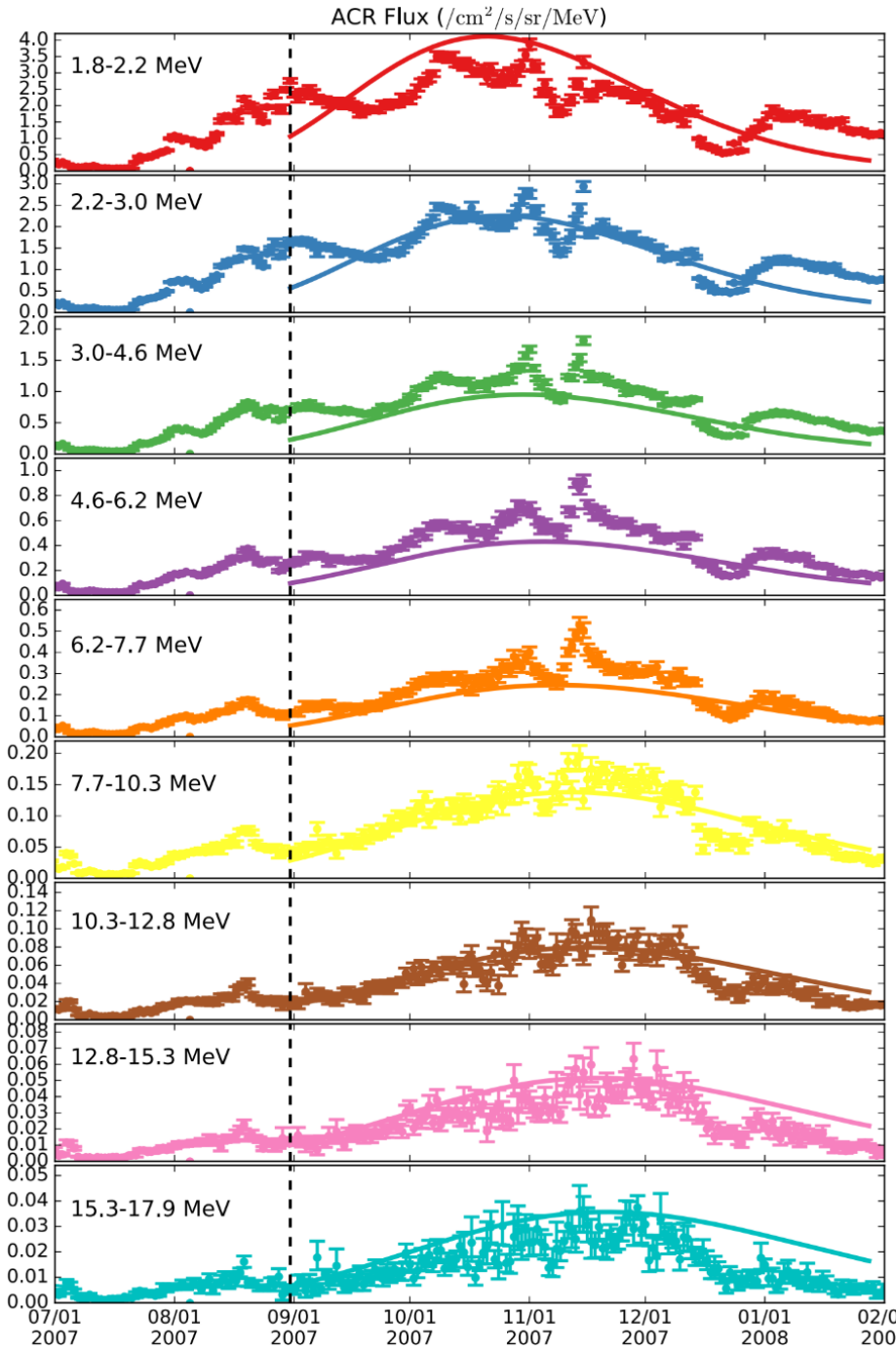

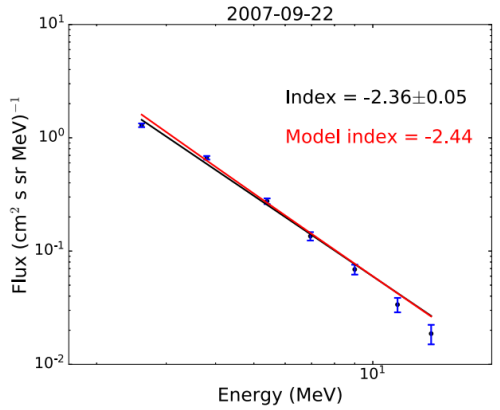

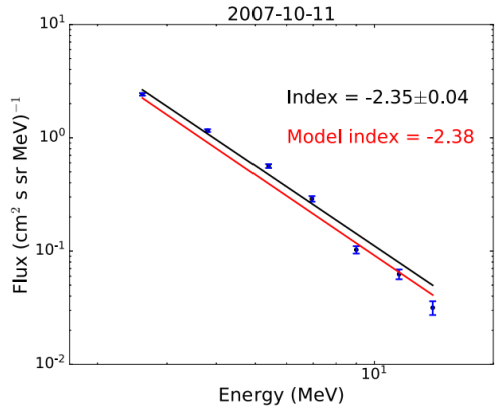

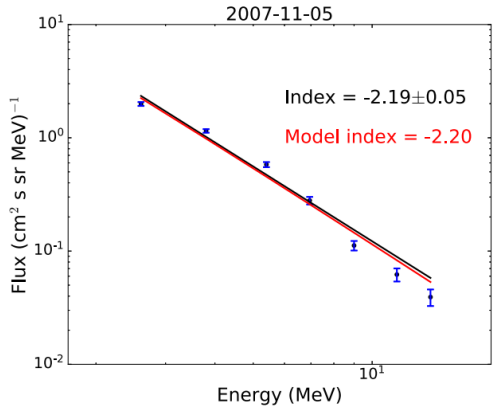

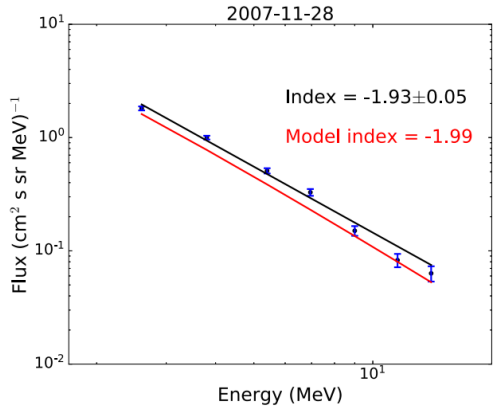

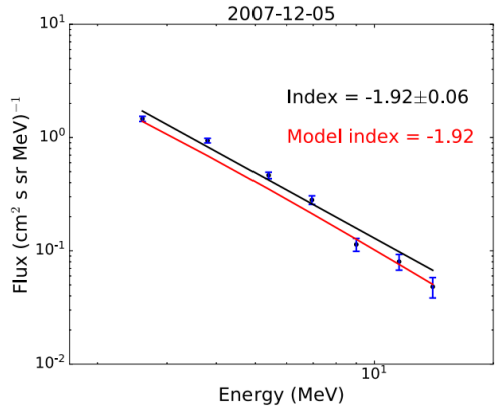

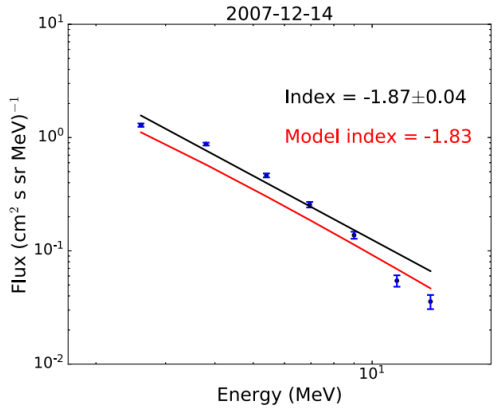

- Observed ACR energetic particle spectrum ~ 100 days after the HTS crossing shows agreement with our reconnection-based stochastic particle acceleration model (Zank et al. 2014, 2015; Zhao et al. 2019b).

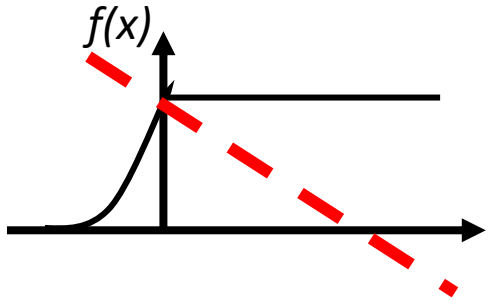

2) How does turbulence interact with shocks? Idealized theory and results[1]

[1]Zank et al., 2021, submitted

2) How does turbulence interact with shocks (and discontinuities more generally)?

Classical problem

- especially in gas dynamics, focus on the amplification of sound (Burgers, 1946; Moore, 1954; Ribner 1954,+)
- extended to MHD in 1960s (Kontorovich, 1959, +, good summary in Anderson, 1963), focus on amplification of sound, but surprisingly done since then, and very little done observationally.

A somewhat systematic study initiated by Pitna et al 2016, 2017, 2021 and Borovsky, 2020 but lacking in theoretical interpretation. The work presented here represents a first step in reexamining this classical problem.

Amplification of upstream spectrum and similarity of upstream and downstream spectra.

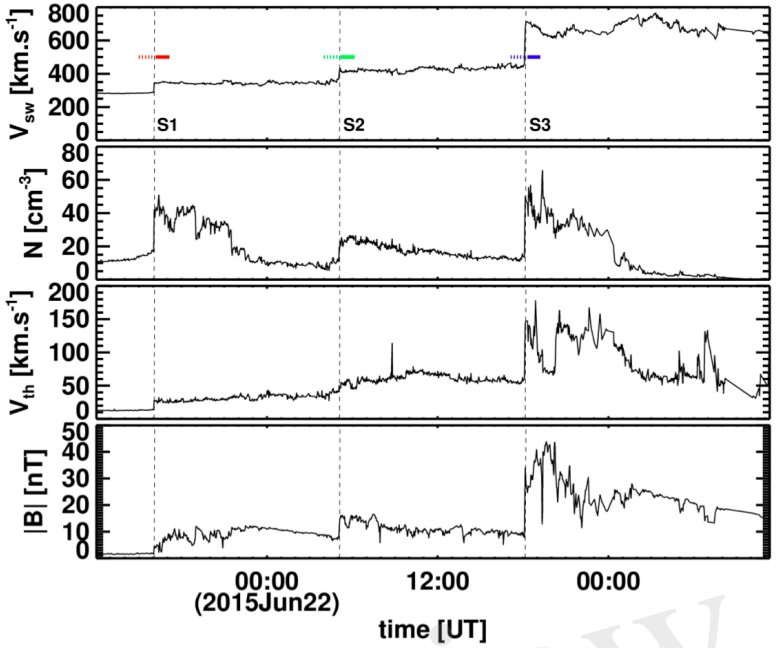

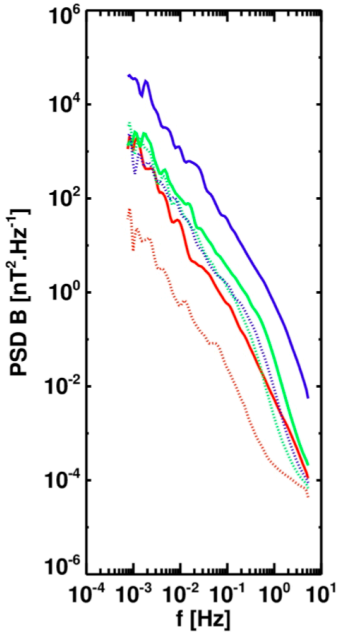

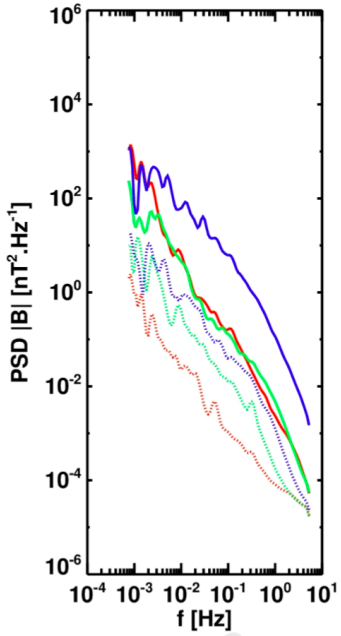

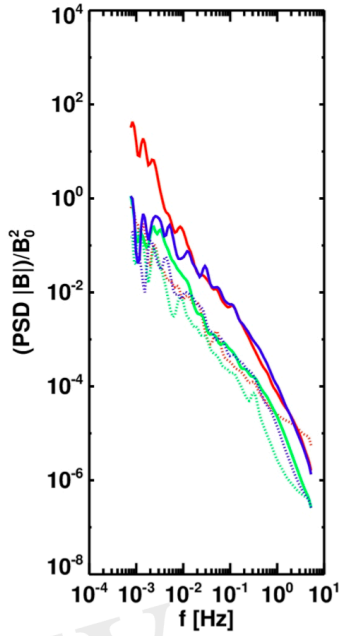

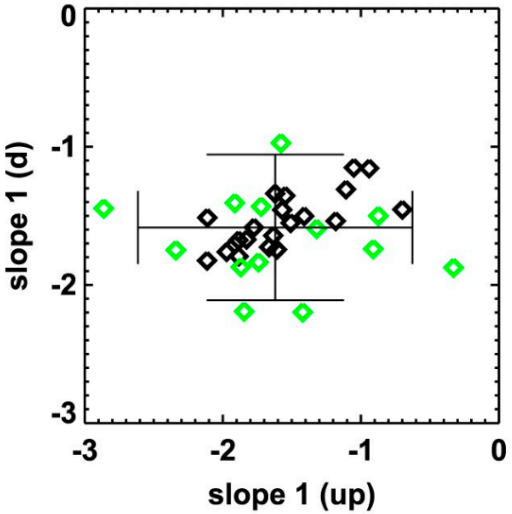

Pitna et al 2016, 2021

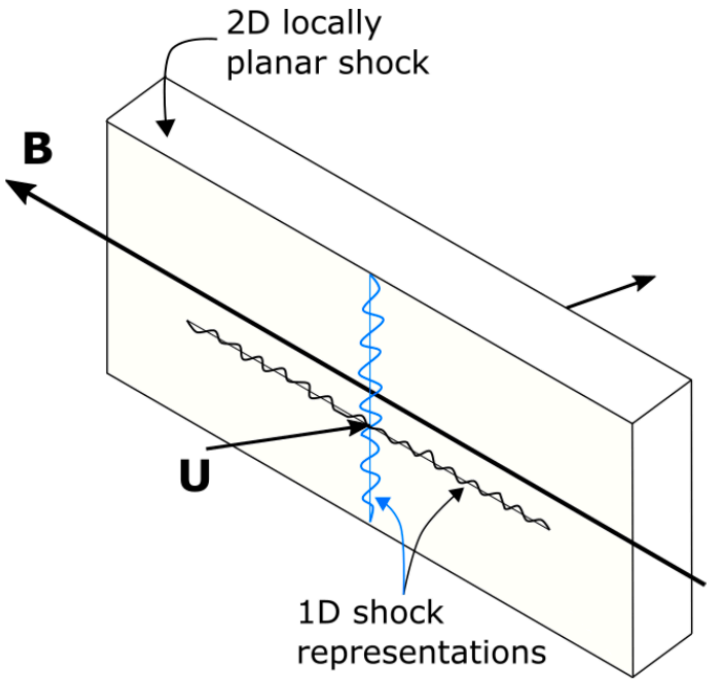

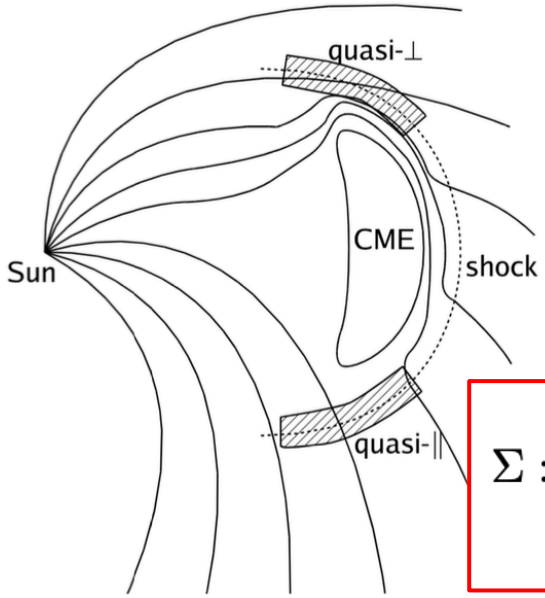

- Need to solve the time-dependent (non-conservation form of the) MHD equations on either side of the shock and then match the solutions across a free boundary (the shock).
- We therefore need to derive the free boundary conditions.

The shock surface and shock normal can be defined by

$$\Sigma : x - \phi(y,z,t) = 0, \qquad \text{and} \qquad \hat{\mathbf{n}} = \frac{(1, -\phi_y, -\phi_z, -\phi_t)}{\sqrt{1+\phi_y^2 + +\phi_z^2 + \phi_t^2}},$$

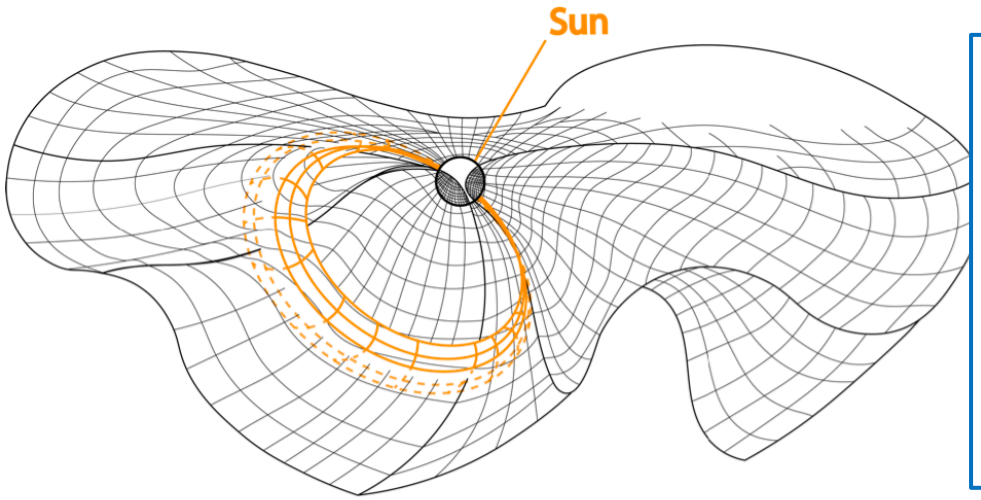

$$\frac{\partial \rho}{\partial t} + \nabla \cdot (\rho \mathbf{U}) = 0;$$

$$\frac{\partial}{\partial t}(\rho \mathbf{U}) + \nabla \cdot \left[\rho \mathbf{U}\mathbf{U} + \left(P + \frac{B^2}{2\mu_0}\right)\mathbf{I} - \frac{1}{\mu_0}\mathbf{B}\mathbf{B}\right] = 0;$$

$$\frac{\partial}{\partial t}\left(\frac{1}{2}\rho U^2 + \frac{P}{\gamma - 1} + \frac{B^2}{2\mu_0}\right) + \nabla \cdot \left[\left(\frac{1}{2}\rho U^2 + \frac{\gamma}{\gamma - 1}P + \frac{B^2}{\mu_0}\right)\mathbf{U} - \frac{1}{\mu_0}\mathbf{U}\cdot\mathbf{B}\mathbf{B}\right] = 0;$$

$$\frac{\partial \mathbf{B}}{\partial t} + \nabla \cdot (\mathbf{U}\mathbf{B} - \mathbf{B}\mathbf{U}) = 0;$$

$$\nabla \cdot \mathbf{B} = 0,$$

- Consider an upstream weak mean magnetic field $\mathbf{B}_0 = B_0\mathbf{z}$ oriented perpendicularly to the flow vector $\mathbf{U}_0 = (U_x, U_y, 0)$, such that transverse magnetic fluctuations $(dB_x, dB_y, 0)$ are of the same order of magnitude as B_0 and thus fluctuations $dB_z << B_0$.
- Can be interpreted as strong perpendicular magnetic turbulence despite the large plasma beta.
- Such an orientation yields magnetic islands in the plane of the flow velocity.

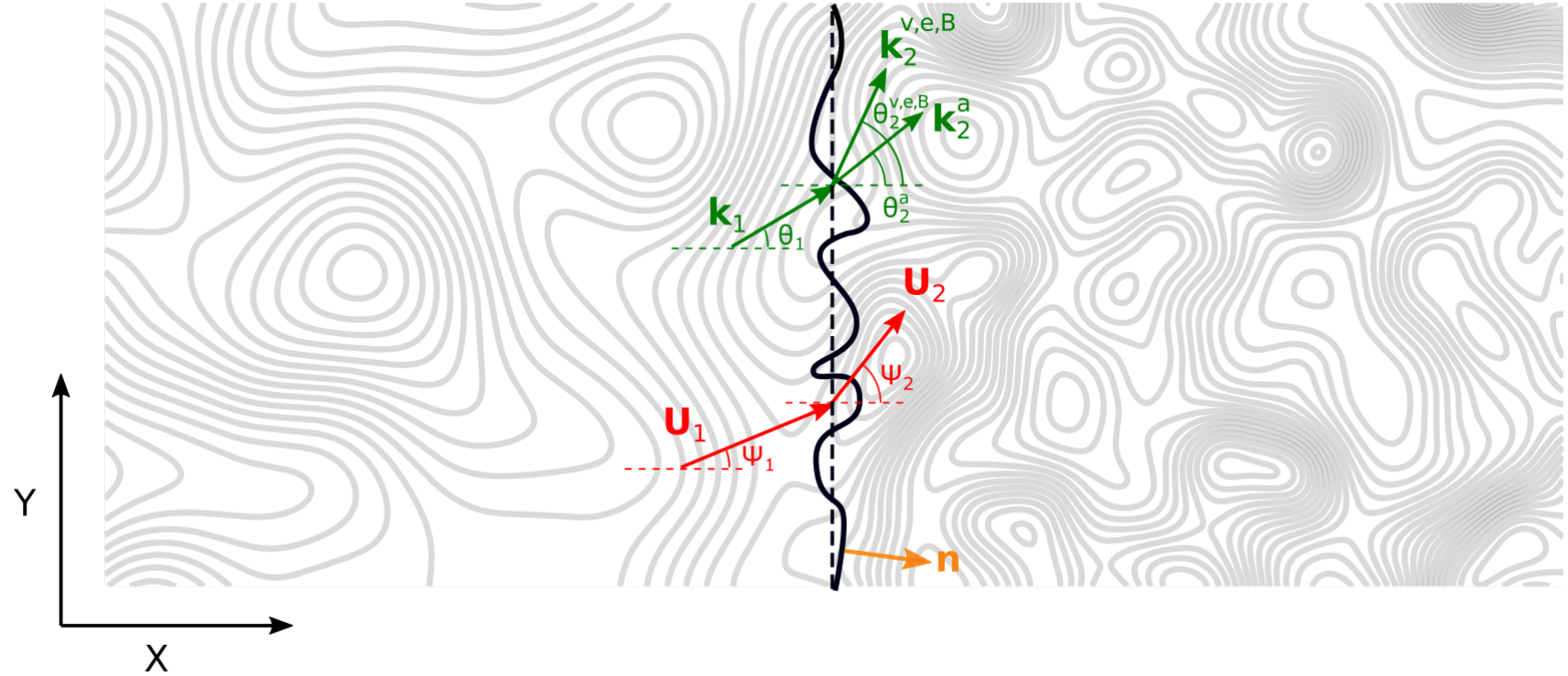

The weak mean magnetic field $\mathbf{B}_0 = B_0\mathbf{z}$ is in/out of the page.

- Can show that the systems cleaves into independent gas dynamic and a magnetic island subsets.
- Find that 3 gas dynamic modes (k_2^a, k_2^v, and k_2^e corresponding to ***acoustic***, ***vorticity***, and ***entropy*** modes) are emitted downstream for an incident gas dynamic mode.
- For an incident magnetic island, a magnetic island k_2^B is transmitted/generated downstream of the shock.

Shock perturbed by a spectrum of small amplitude linearized fluctuations α exp [k.x – ωt] allows us to assume that

$$\phi = \eta \exp\left(i\mathbf{k}\cdot(0,y,z) - \omega t\right),$$

By way of example, focus on conservation of mass – fluctuating shock front yields R-H condition

$$-\phi_t\left[\rho\right] + \left[\rho u_x\right] - \phi_y\left[\rho u_y\right] - \phi_z\left[\rho u_z\right] = 0,$$

Linearizing, applying assumptions yields zeroth-order RH conditions (perpendicular jump conditions):

$$\begin{aligned}
\left[\rho U_x\right] &= 0; \\
\left[\rho U_x^2 + P\right] &= 0; \\
\left[U_y\right] &= 0; \\
\left[\frac{1}{2}U^2 + \frac{\gamma}{\gamma-1}\frac{P}{\rho}\right] &= 0, \\
\left[U_x B_0\right] &= 0, \qquad \text{(higher-order)}
\end{aligned}$$

And the first-order equations for the shock front fluctuation, density, velocity, etc. amplitudes are given by:

$$-\phi_t\left[\rho\right] + m\left[\frac{\delta\rho}{\rho} + \frac{\delta u_x}{U_x}\right] - \phi_y U_y\left[\rho\right] = 0;$$

Recall basic linear modes:

Linearization of equations (16) - (21), assuming $\mathbf{U} = \mathbf{U}_0 + (\delta u_x(x,y), \delta u_y(x,y), 0)$, $\mathbf{B} = \mathbf{B}_0 + (\delta B_x(x,y), \delta B_y(x,y), 0)$ (with $B_0 \sim O(\delta B_x, \delta B_y)$), $\rho = \rho_0 + \delta\rho$, and $P = P_0 + \delta p$, and seeking normal modes $\propto \delta\hat{\Psi} \exp i(\mathbf{k}\cdot\mathbf{x} - \omega t)$ yields the following propagating and advected modes:

(i): *Acoustic modes:* $\omega' = \pm a_0 k$, where $\omega' \equiv \omega - \mathbf{U_0}\cdot\mathbf{k} \neq 0$, with eigenrelations

$$\delta\hat{\rho} = \frac{\delta\hat{p}}{a_0^2}, \qquad \delta\hat{\mathbf{u}} = \mp\frac{\mathbf{k}/k}{\rho_0 a_0}\delta\hat{p}, \qquad \delta\hat{\mathbf{B}} = 0, \qquad a_0^2 = \frac{\gamma P_0}{\rho_0} \quad \text{(sound speed)}. \tag{22}$$

(ii): *Entropy modes:* $\omega' = 0$ with eigenrelations

$$\delta\hat{s} = -\frac{\gamma\delta\hat{\rho}}{\rho_0}, \qquad \delta\hat{p} = 0, \qquad \delta\hat{\mathbf{u}} = 0, \qquad \delta\hat{\mathbf{B}} = 0, \qquad \delta\hat{\rho} \quad \text{arbitrary}.$$

(iii): *Vortical modes:* $\omega' = 0$, with eigenrelations, after introducing $\mathbf{k} = k(\cos\theta, \sin\theta) \equiv k(\alpha, \beta)$,

$$\delta\hat{p} = 0, \qquad \delta\hat{\mathbf{B}} = 0, \qquad \delta\hat{\rho} = 0, \qquad \delta\hat{\mathbf{u}} \neq 0, \qquad \delta\xi_z \neq 0;$$
$$\mathbf{k}\cdot\delta\hat{\mathbf{u}} = 0 \Longrightarrow \delta\hat{\mathbf{u}} = \delta\hat{u}(-\beta, \alpha).$$

(iv): *Magnetic island modes:* $\omega' = 0$, with

$$\delta\hat{\rho} = 0, \qquad \delta\hat{p} = 0, \qquad \delta\hat{\mathbf{u}} = 0, \qquad \delta\hat{\mathbf{B}} \neq 0, \qquad \delta J_z \neq 0;$$
$$\mathbf{k}\cdot\delta\hat{\mathbf{B}} = 0 \Longrightarrow \delta\hat{\mathbf{B}} = \delta\hat{B}(-\beta, \alpha).$$

Transmission of incident vortical modes:

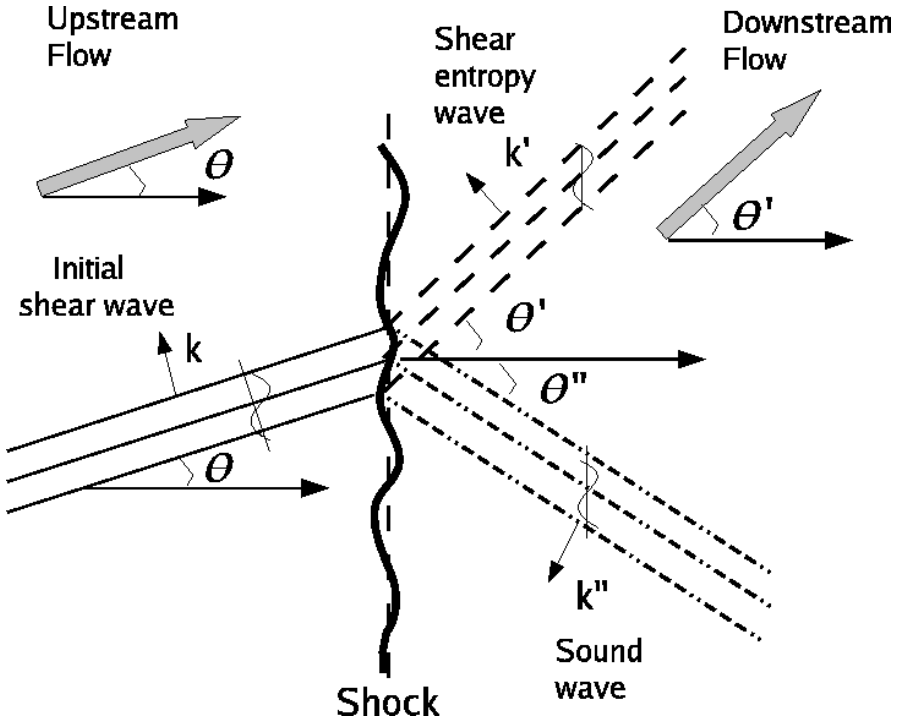

Rewrite all downstream variables in terms of the diverging fluctuations:

$$\delta\hat{\rho}_2 = \delta\hat{\rho}_2^a + \delta\hat{\rho}_2^e + \delta\hat{\rho}_2^v = \delta\hat{\rho}_2^a + \delta\hat{\rho}_2^e = \frac{\delta\hat{p}_2}{a_2^2} + \frac{\rho_2}{\gamma}\delta\hat{s}_2;$$

$$\delta\hat{u}_{x2} = \delta\hat{u}_{x2}^a + \delta\hat{u}_{x2}^v = \pm\frac{\cos\theta_2^a}{\rho_2 a_2}\delta\hat{p}_2 - \sin\theta_2^v\delta\hat{u}_2,$$

- To determine downstream angles for transmitted and generated modes resulting from upstream vortical mode, we can assume that the frequency ω and tangential wave number k_y are continuous across the *O(1)* shock, i.e., $\omega_1 = \omega_2 = \omega$ and $k_{y1} = k_{y2} = k_y$.
- Solving $\omega'_1 = 0$ and either $\omega'_2 = 0$ (downstream vorticity or entropy mode) or $\omega'_2 = +/-a_0k_2$ (downstream sound wave) yields angles for transmitted/generated modes:

$$\tan\theta_2^v \equiv k_y/k_{x2} = \frac{U_{x2}}{U_{x1}}\tan\theta_1^v = r^{-1}\tan\theta_1^v,$$

$$\cot\theta_2^a = k_{x2}/k_y = -\frac{rM_2^2\cos^2\psi_2}{1-M_2^2\cos^2\psi_2}\cot\theta_1^v \pm \frac{1}{\sqrt{1-M_2^2\cos^2\psi_2}}\left(\frac{r^2M_2^2\cos^2\psi_2}{1-M_2^2\cos^2\psi_2}\cot^2\theta_1^v - 1\right)^{1/2},$$

Notices that the downstream acoustic wave field is confined to propagation angles for which the discriminant is >= 0, otherwise waves evanescent downstream. Slightly weaker condition holds:

$$\tan^2\theta_1 < r^2M_2^2\cos^2\psi_2,$$

Fluctuating kinetic, density, and magnetic energy amplification and spectra

- **Solutions to linearized b.c.'s for the fluctuating velocity, density, and magnetic field amplitudes as functions of the incident flow angle.**
- Energies in the acoustic, vorticity, entropic, and magnetic island modes considered as separate transmission problems for upstream vorticity, entropy, and acoustic fluctuations.
- Consider two canonical cases that resemble a high plasma beta shock: a *quasi-aligned* case and a *quasi-perpendicular* case in terms of the incident flow vector. Parameters ensures that both shocks have the same compression ratio *r = 3.30.*

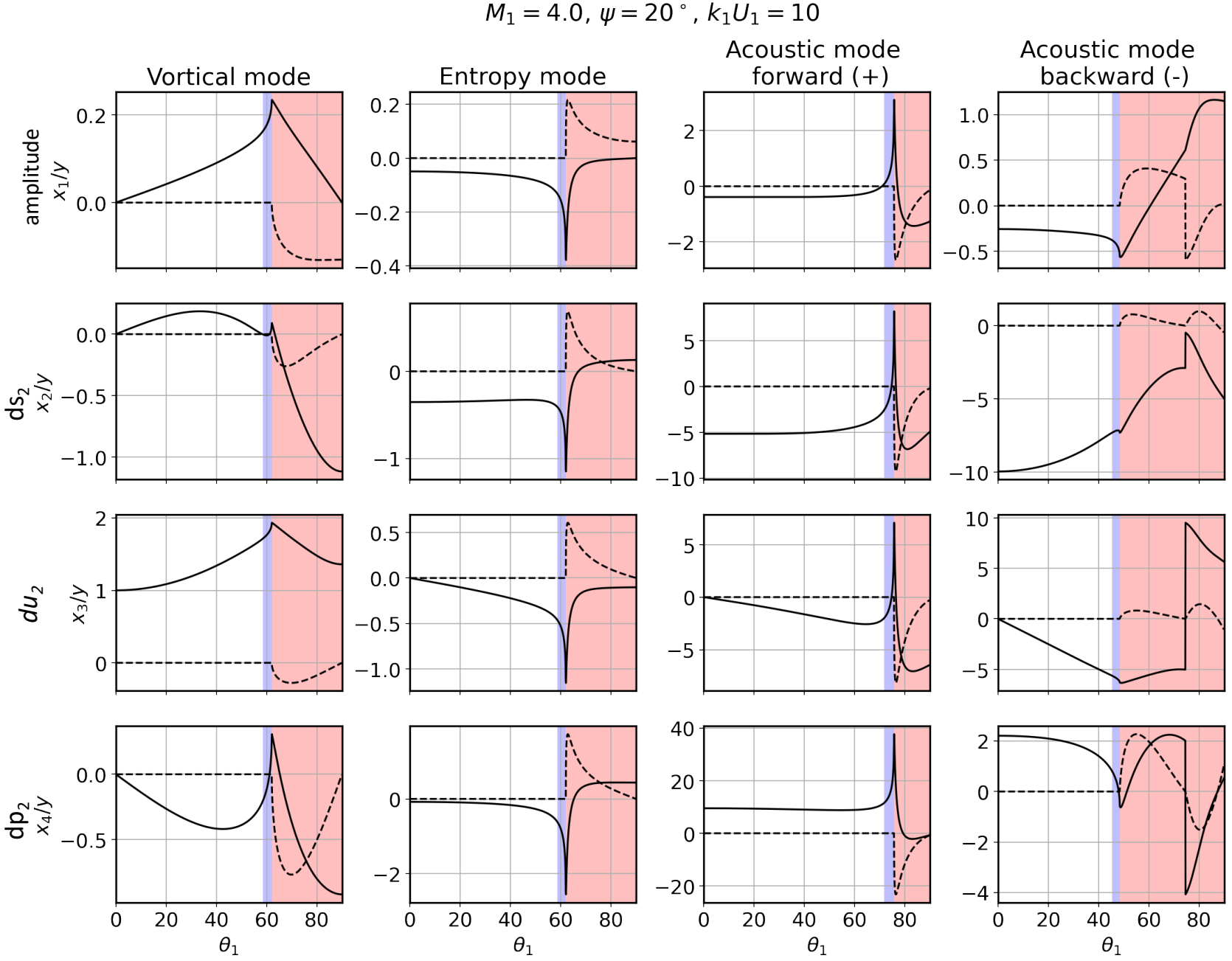

Velocity variance of transmitted fluctuations $M_1 = 4.0,\ \psi = 20^\circ,\ \overline{k_1 U_1} = 10$

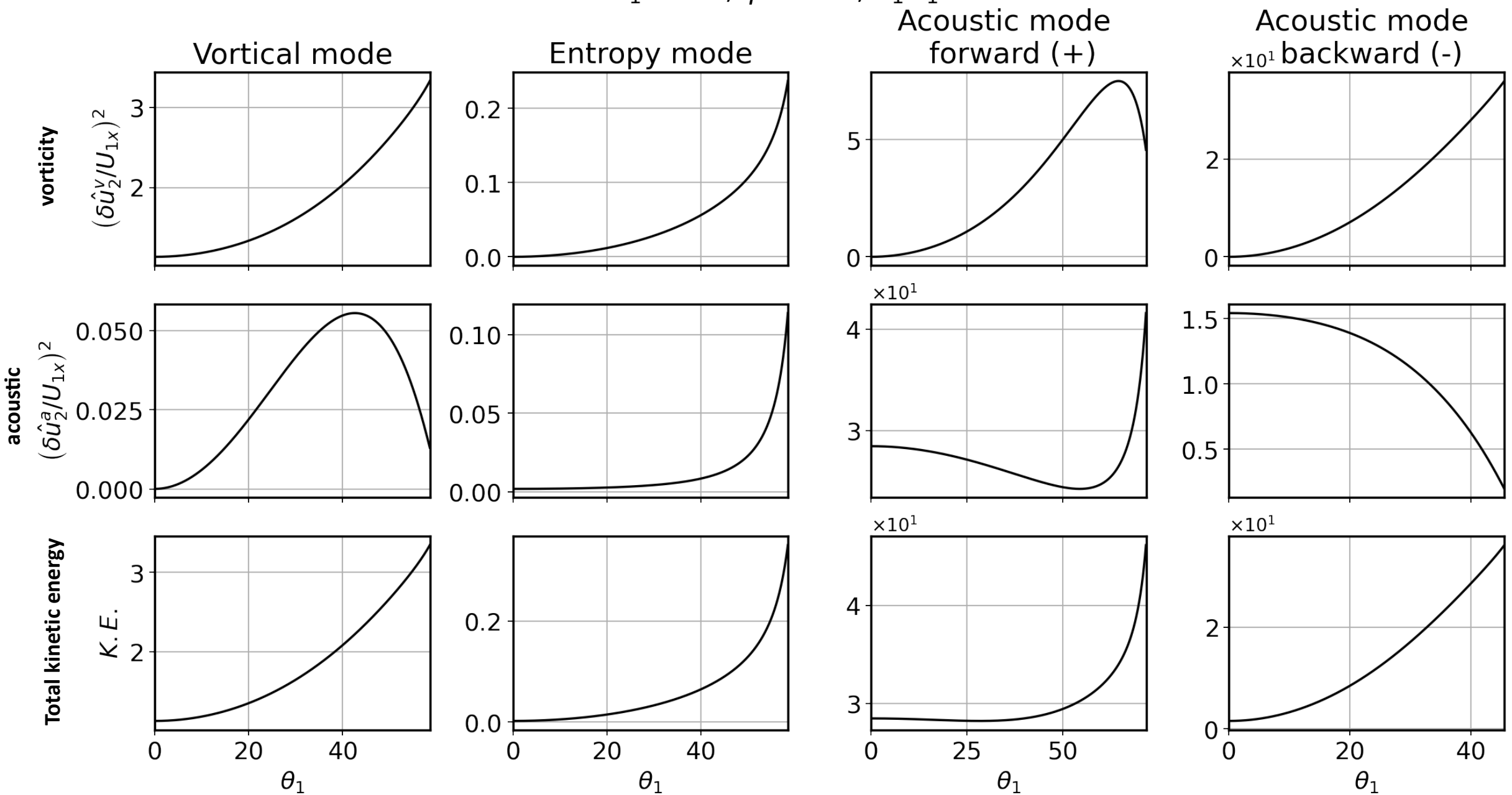

Density variance of transmitted fluctuations

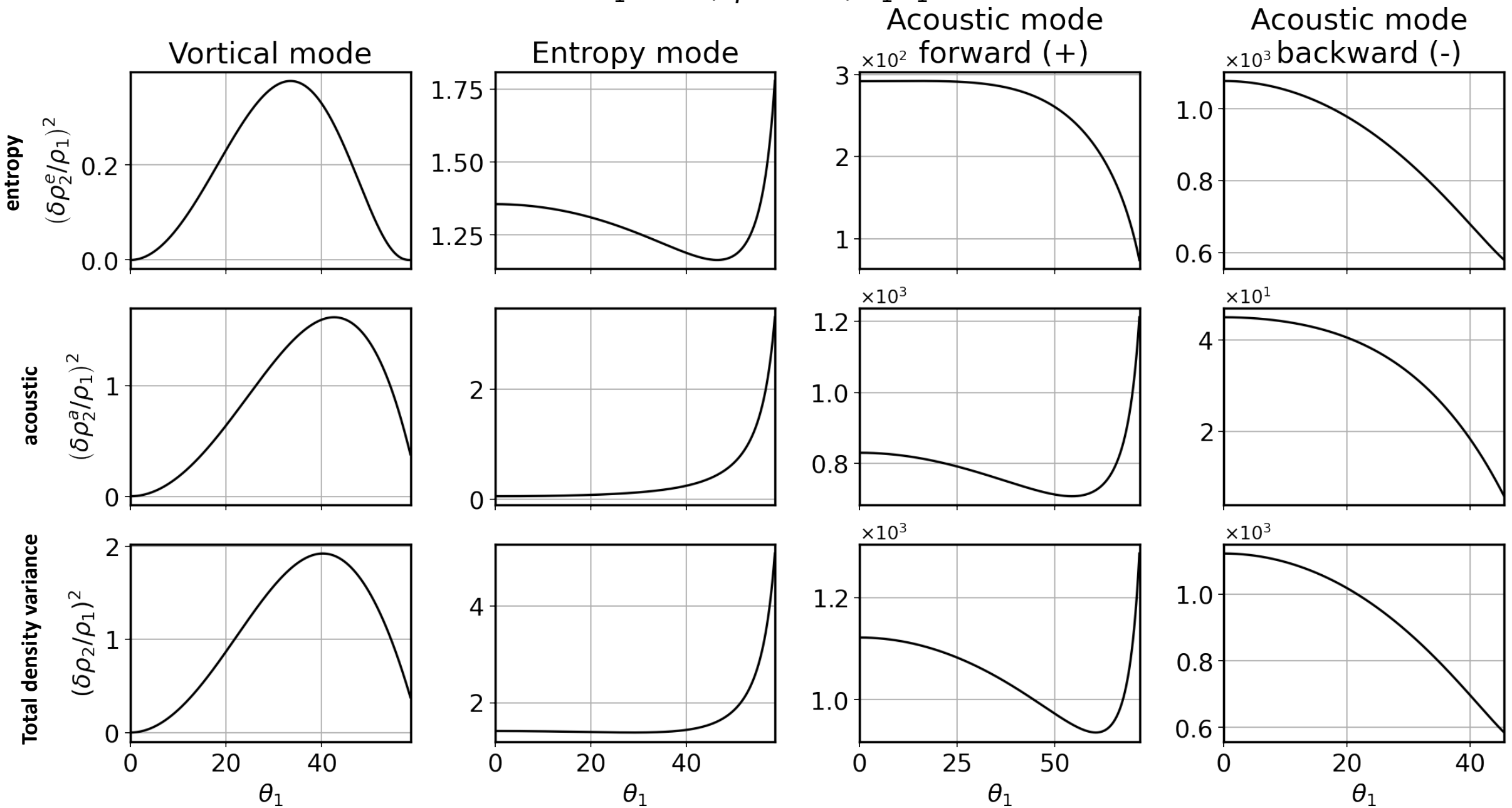

Transmission of upstream magnetic islands or flux ropes

- Magnetic modes fully decoupled from the gas dynamic fluctuations in high plasma beta regime
- As before, $\omega_1' = 0$ and $\omega_2' = 0$, giving

$$\tan\theta_2^B = k_y/k_{x2} = \frac{U_{x2}}{U_{x1}}\tan\theta_1^B,$$

- Downstream flux rope amplitude given by

$$\delta\hat{B}_2 = r\frac{\cos\theta_1^B}{\cos\theta_2^B}\delta\hat{B}_1 = \frac{\sin\theta_1^B}{\sin\theta_2^B}\delta\hat{B}_1,$$

where $\delta\hat{\mathbf{B}} = \delta\hat{B}(-\beta,\alpha),$

- Amplification of magnetic islands relatively modest but independent of shock obliquity.

- Transmission of an upstream spectrum of magnetic island fluctuations with assumed spectral form

$$E(k) \propto (\delta X_i)^2\, k \propto \frac{1}{1+(k\ell)^\nu},$$

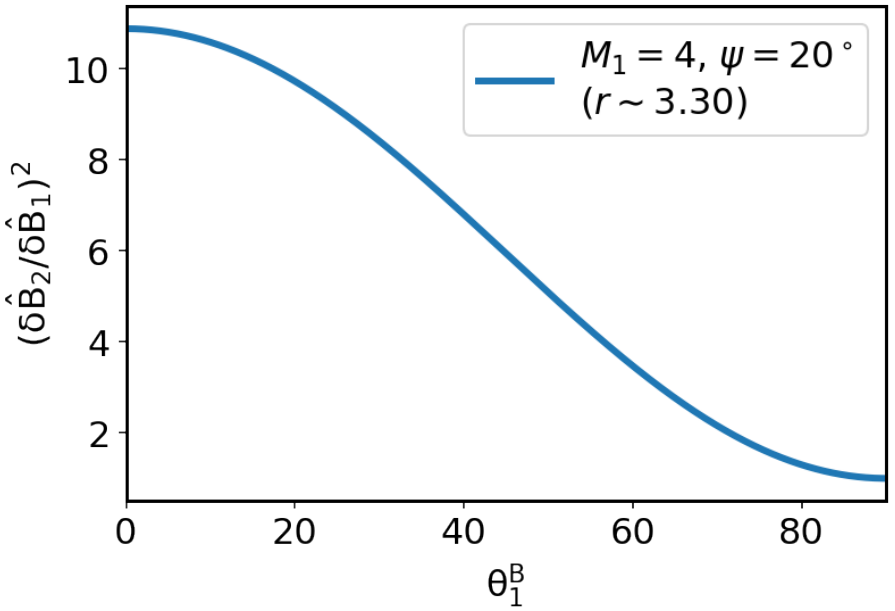

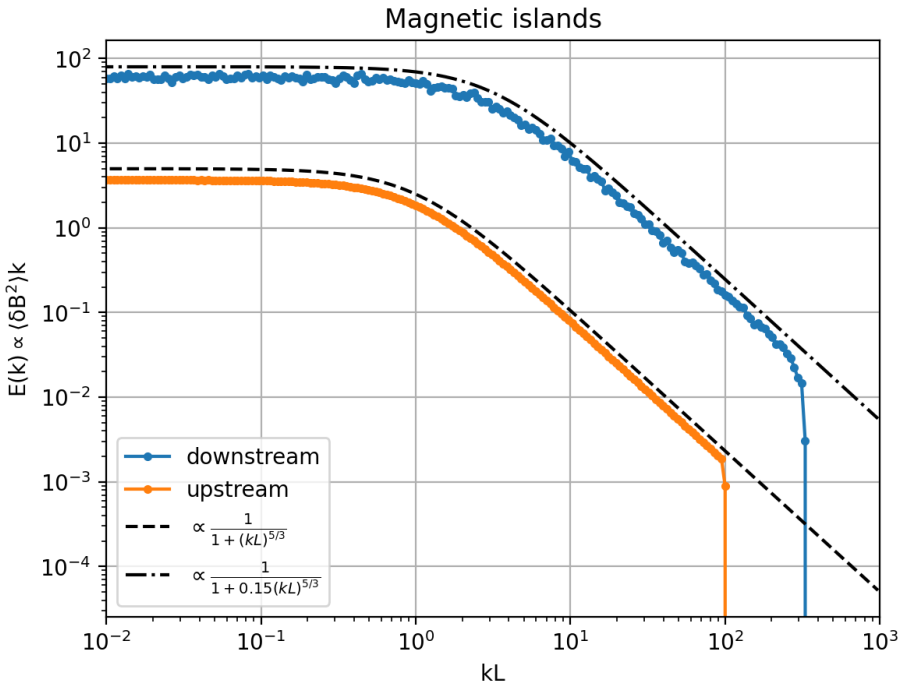

Downstream spectra generated by incident vortical, entropy, and acoustic fluctuations:

$$E(k) \propto (\delta X_i)^2 \, k \propto \frac{1}{1+(k\ell)^{\nu}},$$

1) For the upstream spectrum, we prepare a number of waves assuming omni-directional power spectrum with θ_1 randomly distributed from 0 to $\pi/2$ (orange curve);
2) we calculate θ_2 and the amplitudes for each of the vortical, entropy, and acoustic modes transmitted or generated downstream for each incident wave, and
3) we calculate the power spectrum of the downstream waves in k-θ_2 space for each of the generated modes and then integrate over θ_2 to obtain the downstream omni-directional power spectrum (blue curve).

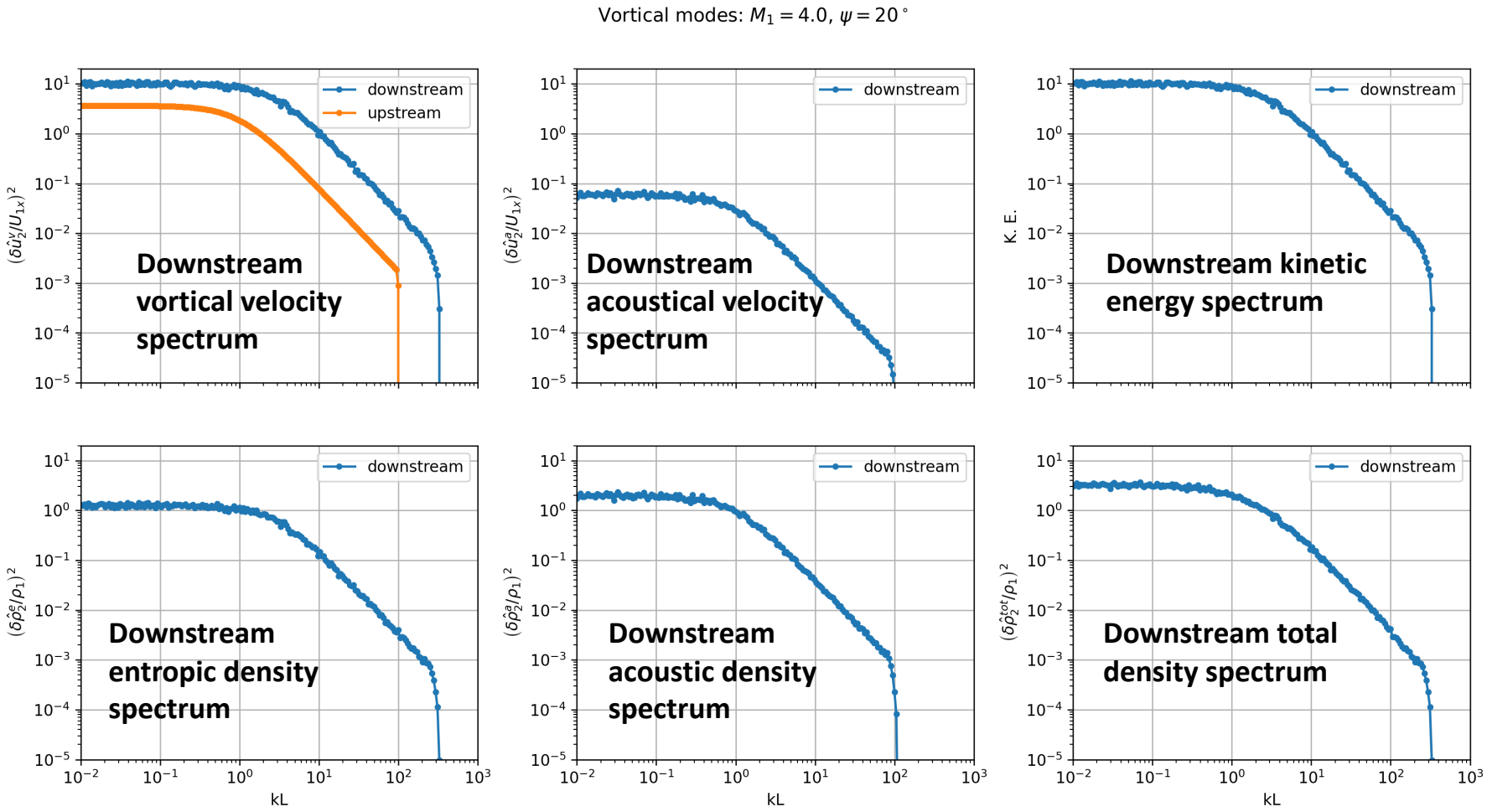

Incident spectrum of vortical modes

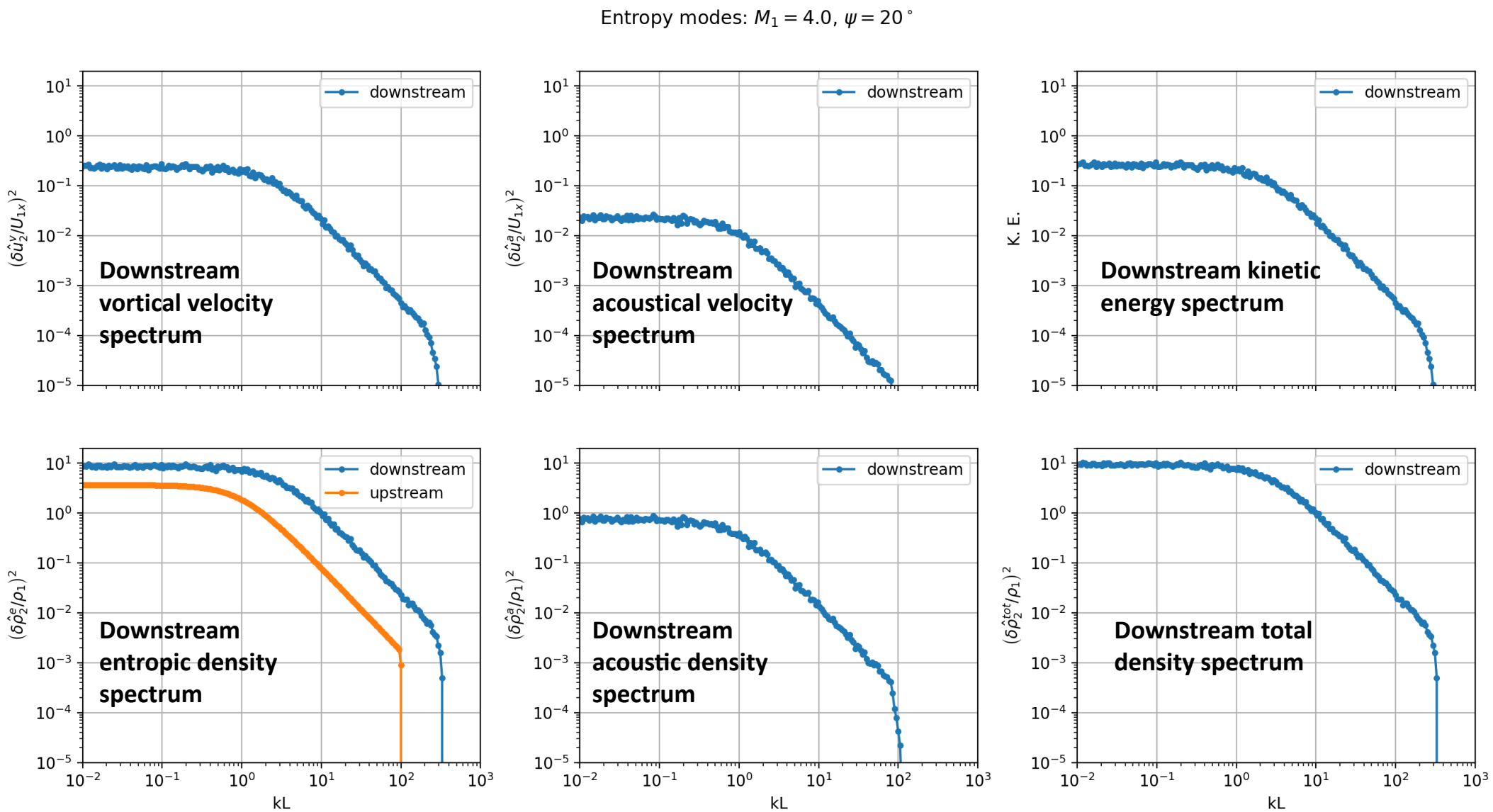

Incident spectrum of entropy modes

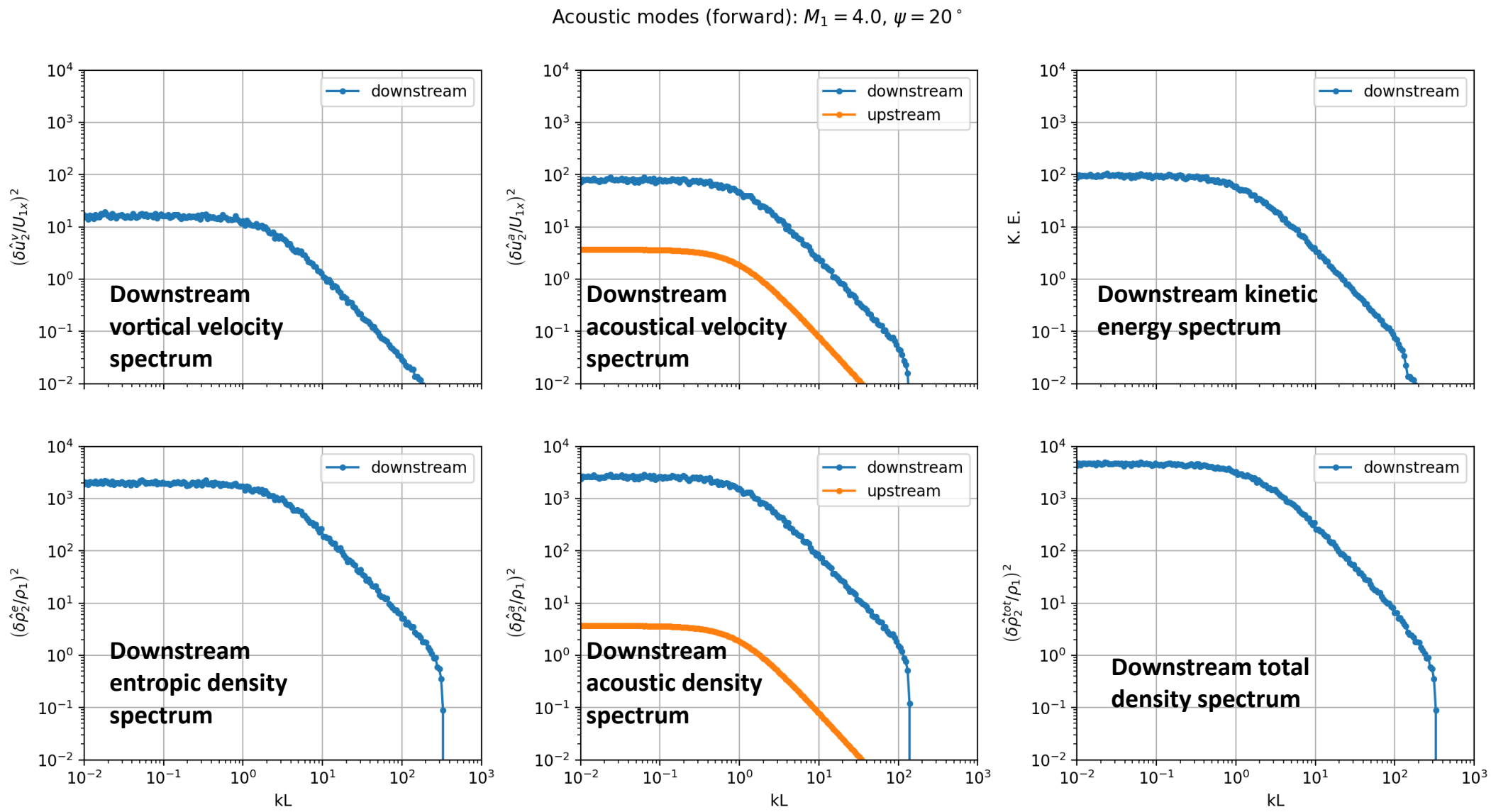

Incident spectrum of forward acoustic modes

3) Comparison of (idealized) theory with heliospheric observations[1]

[1]Zank et al., 2021, submitted

3) Comparison of (idealized) theory with heliospheric observations

Consider 3 quasi-perpendicular shocks observed at 1 au (*Wind*), 5 au (*Ulysses*), and 84 au (*Voyager 2*)

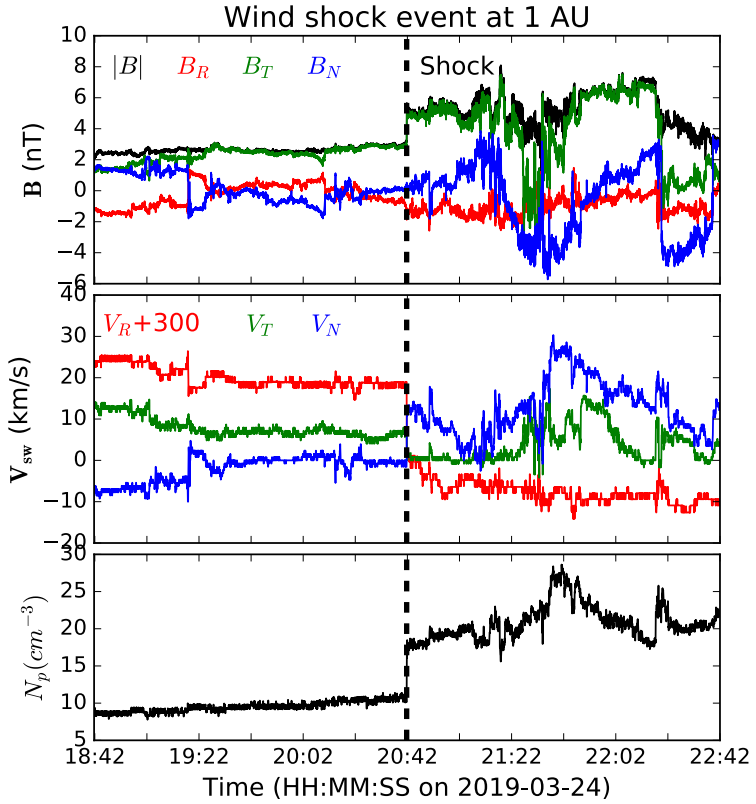

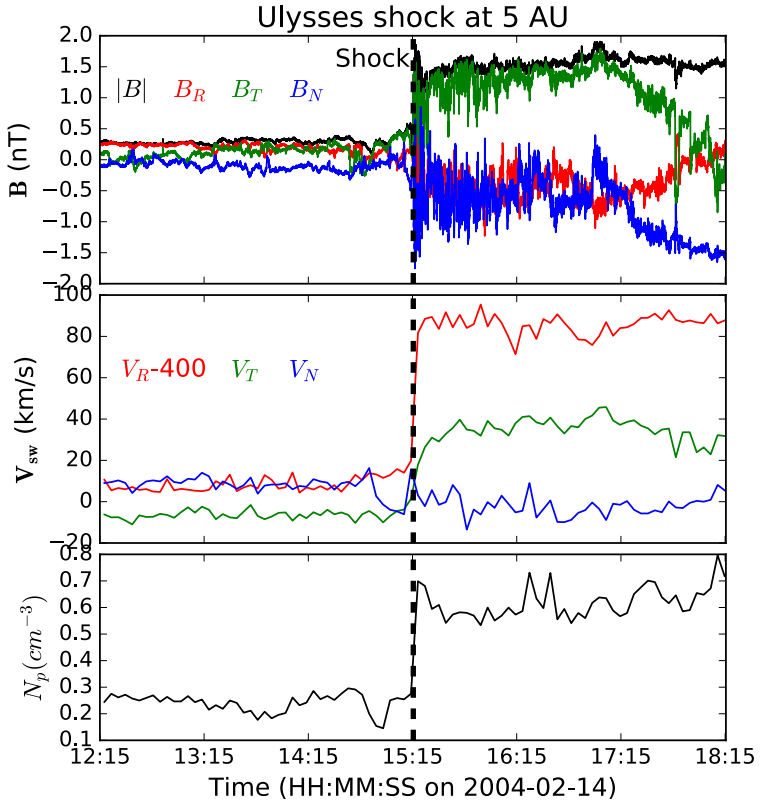

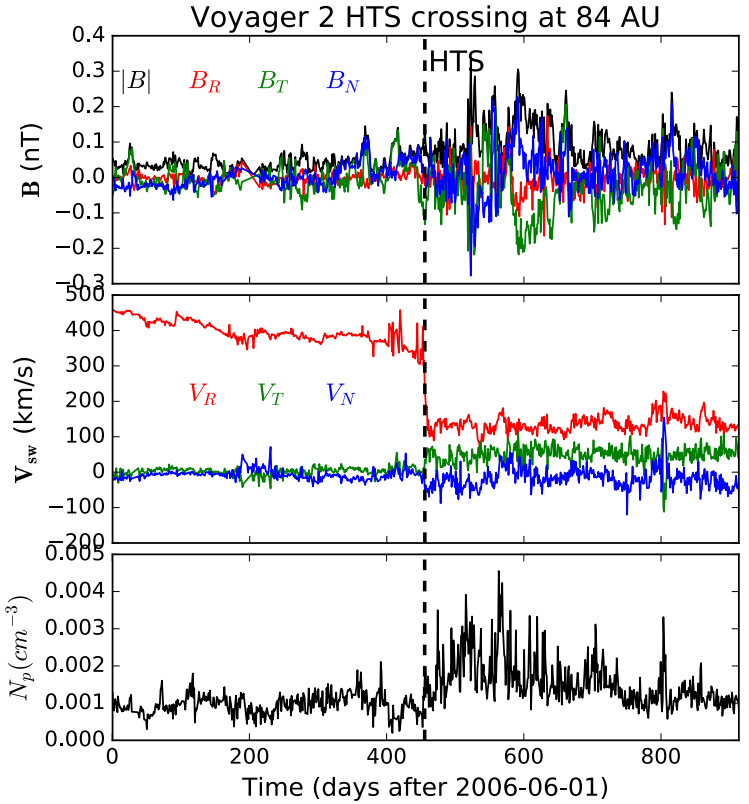

Zhao et al. (2019a, 2019b) investigated Ulysses and Voyager 2 events in context of magnetic flux ropes that were identified upstream and downstream of shock

	position [au]	Shock Angle Ψ_1 [°]	Mach Number M_1	compression ratio
Wind	1	80	11	2.22
Ulysses	5	53	3.8	2.55
Voyager 2	84	10	1.82	2.73

Are the assumptions inherent in theory consistent with observations?

1) **Relative strength of fluctuating magnetic field to the upstream mean magnetic field**: (1) *Wind* event: $\delta B/B_0$ = 0.54 and $\delta B_\perp/B_0$ = 0.5; (2) *Ulysses* event: $\delta B/B_0$ = 0.68 and $\delta B_\perp$/B0 = 0.59, and (3) *Voyager 2* event: $\delta B/B_0$ = 12.47 and $\delta B_\perp/B_0$ = 10.

ANS: $B_0 \sim O(\delta B)$ is reasonable assumption for the three events. Values of the ratio $\delta B_\perp/B_0$ indicate most of **power resides in the 2D magnetic field fluctuations**. Further confirmed by computing $\langle \delta B_{2D}^2 \rangle / \langle \delta B_{slab}^2 \rangle$ and $\langle \delta U_{2D}^2 \rangle / \langle \delta U_{slab}^2 \rangle$ upstream and downstream of each event finding values >> 1 [e.g., Wind: 23.76 (δB, up), 7.14 (δB, down), 15.96 (δU, up), 103.71 (δU, down)].

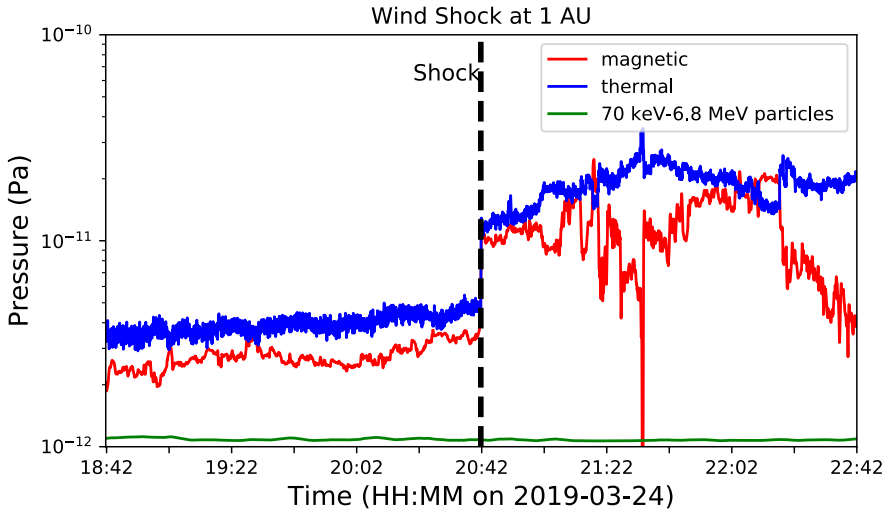

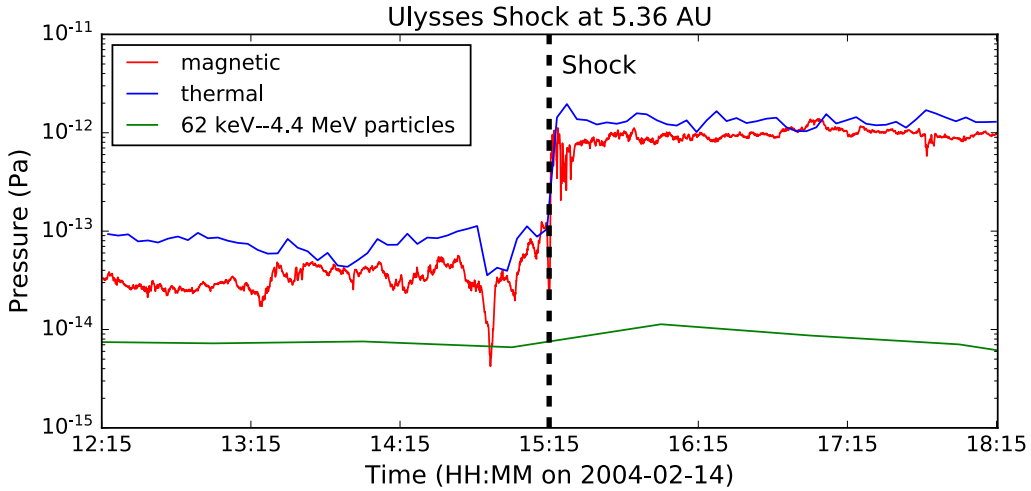

2) **Plasma beta > 1?:** Thermal pressure exceeds magnetic pressure for *Wind* and *Ulysses* shocks, so plasma beta ~1.5 to 3. Energetic particle pressure at HTS (anomalous cosmic rays, pickup ions) dominates upstream thermal and magnetic field pressure e.g., Decker et al., 2008, implies plasma beta >> 1. **ANS:** Yes, beta > 1.

Based on Wind, Ulysses, and Voyager 2 parameters, the underlying assumptions in the analysis are met reasonably well and can therefore compare the observed downstream spectra for the three shocks theoretical predictions with some confidence.

Observed and predicted magnetic spectra

Power spectrum analysis performed for each shock event using different time interval lengths, which represents roughly the inertial range of turbulence at different radial distances. Observed upstream magnetic variance spectrum used for the source terms in theory.

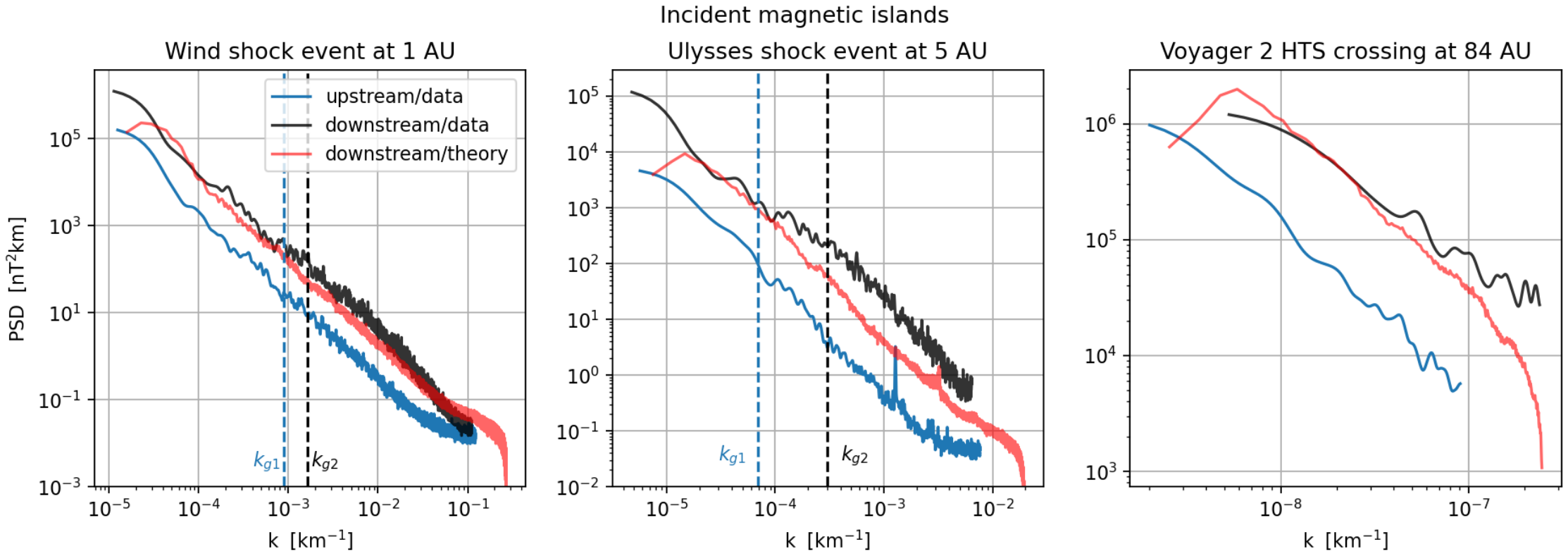

Comparison of the theoretical and observed downstream magnetic variance spectra for all three cases is excellent. Enhancement in downstream spectral intensity and the spectral slope well captured by theory with only noticeable discrepancy occurring in the dissipation range of the downstream Ulysses spectrum with some excess power.

Why should the transmission problem for magnetic turbulence agree so well with observations?

- Despite the idealized character of the theory and its restriction to magnetic islands, the reason for the good correspondence with the observed downstream PSDs likely stems from the two-component nature of solar wind turbulence.

- In this paradigm, for which there is both theoretical and observational support, solar wind turbulence is a superposition of a dominant quasi-2D component and a minority slab component (the quasi-2D-slab model of nearly incompressible (NI) MHD).

- The theory of turbulence transmission through a shock wave presented here describes the transmission of the dominant 2D component, and hence it is not altogether surprising that the theory accounts accurately for the observed downstream spectrum.

Observed and predicted kinetic energy and density spectra

- Only *Wind* plasma data of sufficient resolution used to determine kinetic energy and density variance spectra upstream and downstream of the shock.
- Unlike the magnetic variance case, we must consider source terms corresponding to incident vortical fluctuations, incident entropy fluctuations, and incident forward and backward acoustic fluctuations i.e., a superposition of the source terms.

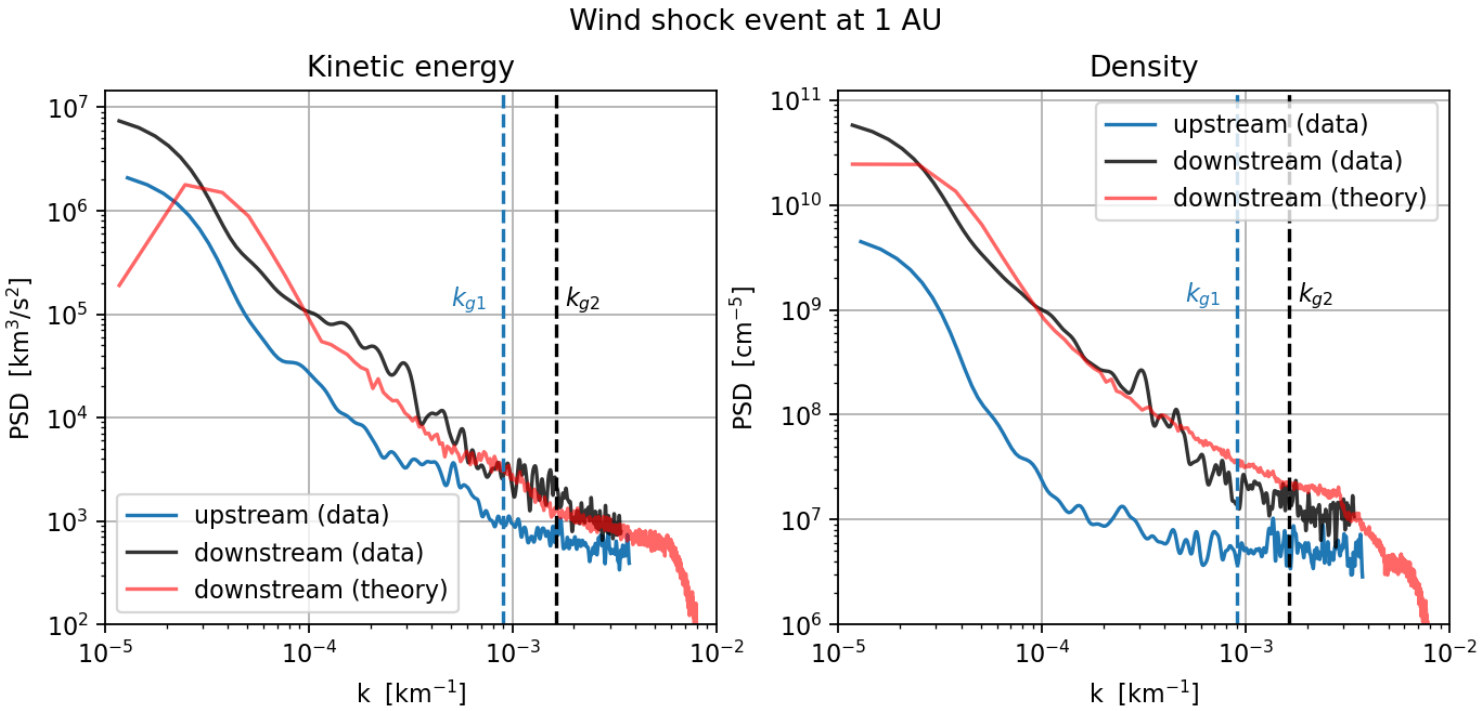

- Need the relative contribution of each observational mode to the kinetic energy and density spectra. The ratio of the 2D to slab energy in velocity fluctuations for Wind is $\langle \delta U_{2D}^2 \rangle / \langle \delta U_{slab}^2 \rangle = 15.96 \sim 16$. Use as proxy for energy in incompressible quasi-2D (vortical) and compressible (acoustic) fluctuations to decompose observed upstream kinetic energy and density variance spectra into vortical and acoustic kinetic modes and entropy and acoustic density fluctuations.
- Thus, we assume that the upstream velocity and density fluctuations are primarily vortical and entropy (incompressible) modes instead of acoustic (compressible) modes. Consistent with the quasi-2D-slab superposition model.

4) Concluding remarks

- Despite the idealized formulation, we apply the theoretical shock-turbulence transmission problem to shocks observed at 1 au, 5 au, and 84 au. In each case, the ordering $B_0 \sim O(\delta B)$ holds and fluctuating magnetic field component dominated by the $\delta B_\perp$, validating the application of the theory to the observations.
- Since solar wind turbulence appears to be well described as a superposition of a dominant 2D component and a minority slab component, we consider the transmission of dominant quasi-2D turbulence across a shock while neglecting the minority component.
- We took observed upstream magnetic spectrum and computed theoretical downstream spectrum and compared to observed downstream spectrum. Agreement between predicted and observed downstream magnetic variance spectrum remarkably good, matching spectral amplitude and spectral form and slope for all three cases.
- Only *Wind* shock had plasma data of sufficient resolution to allow comparison of observed and theoretical kinetic energy and density variance spectra.
- Observed Wind ratio of quasi-2D to slab energy motivates decomposition of upstream fluctuations into primarily incompressible 2D modes, i.e., magnetic islands, vortical and entropy modes, and a smaller acoustic component.
- Complicated superposition of different downstream transmitted and generated compressible and incompressible fluctuations yields the theoretically predicted spectrum that results in very satisfying agreement with observations.

This gives us some confidence that

i) solar wind turbulence is comprised primarily of a majority quasi-2D component, and

ii) the linear free boundary theory presented here describes accurately the transmission of turbulence across collisionless quasi-perpendicular shocks.

Final thoughts if time permits

5) Some final thoughts about the evolution of turbulence behind a shock:

Pitna et al 2017 observations; Zank et al 2002 (simple) theory; Nakanotani et al 2020 simulations

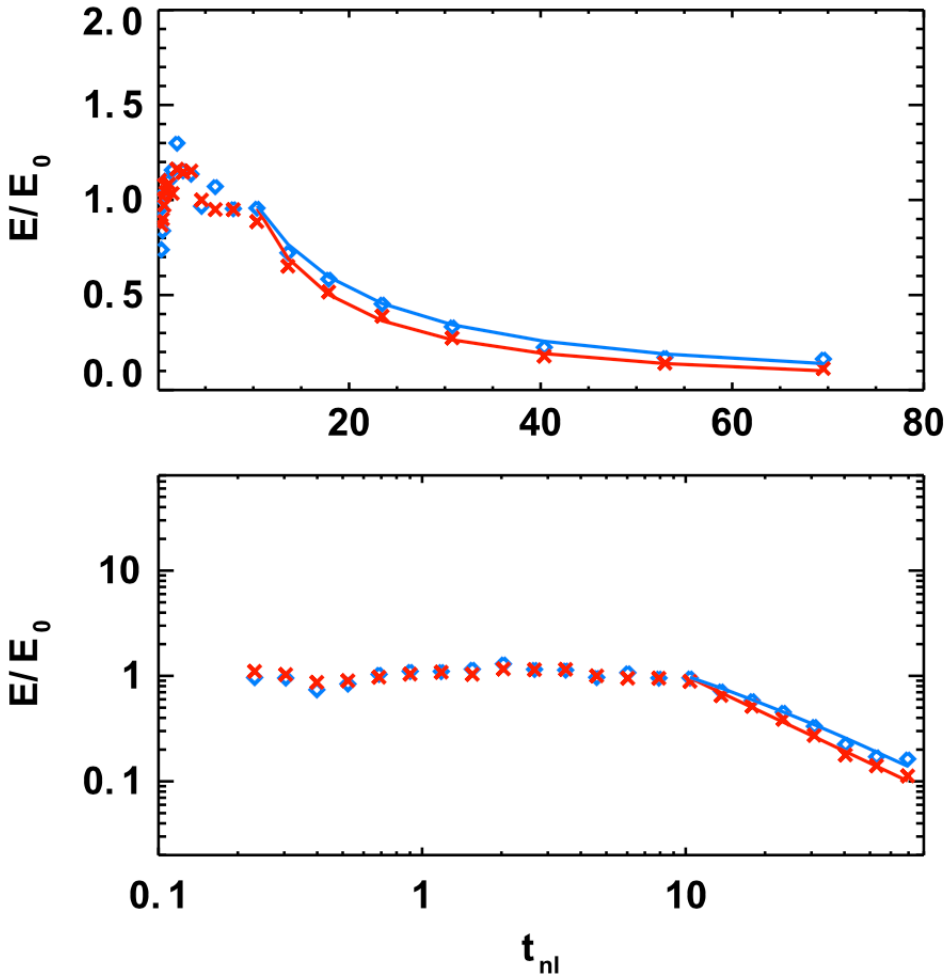

Normalization ($E_{k,0}$, $E_{b,0}$) immediately downstream of the shock.

- Decay of normalized kinetic (red crosses) and magnetic (blue circles) energy behind interplanetary shocks (Pitna et al 2017, superposed epoch analysis) plotted as function of nonlinear time t_{nl}.
- Averages show decreasing trends in both energies but trend not monotonic – initial increase of both energies (up to t_{nl} ~ 2), constant value up to t_{nl} ~ 10, followed by decay for larger times.
- Pitna et al consider model function form (Biskamp 2003)

$$E(t_{nl}) = \left(\frac{t_{nl} - t_0}{t_d - t_0} \right)^n,$$

- For magnetic energy decay, t_0 = -4 +/- 2 and n = -1.2 +/- 0.1. For kinetic energy decay, t_0 = 0 +\- 2 and n = -1.2 +\- 0.1.

- Not unlike decay of turbulence behind grid in wind tunnel experiments a la Batchelor.

Nakanotani et al 2020: 2D Hybrid Simulation

Geometry and Parameters

- Force free condition
- Density and |B| is uniform

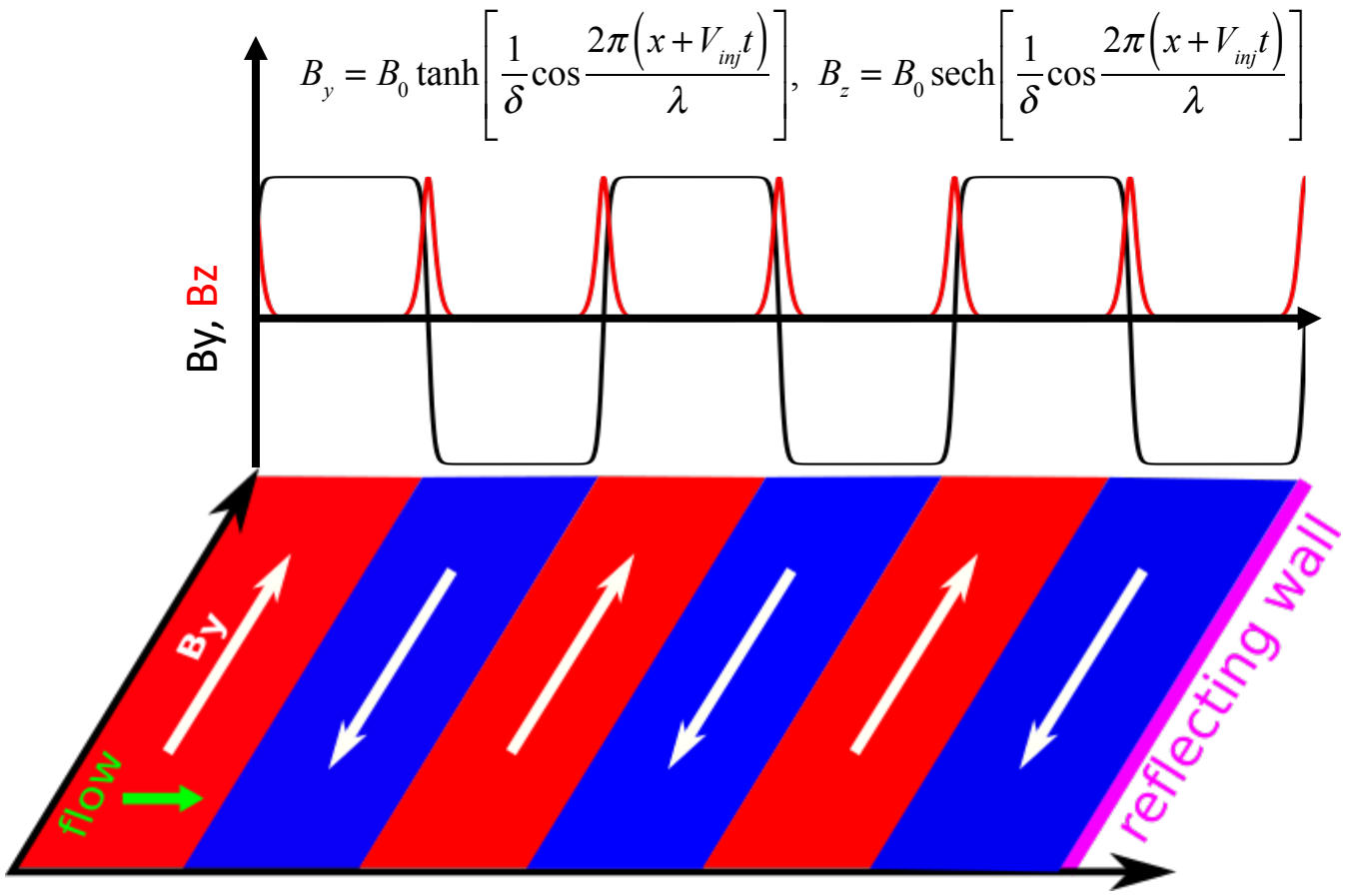

[Sironi & Spitkovsky, 2011, Burgess et al. 2016]

Normalization

- Length --> c/ω_{pi}
- Time --> Ω_i^{-1}
- Velocity --> V_A (Alfvén velocity)

$M_{A,inj}$	2
$\beta_i=\beta_e$	0.5
δ	0.1
λ	50 c/ω_{pi}
ppc	100
L_x x L_y	200 x 204.8 c/ω_{pi}
$\Delta x=\Delta y$	0.2 c/ω_{pi}
Δt	0.01 Ω_i^{-1}

Results: Animation of the Interaction of Current Sheets with a Shock Wave

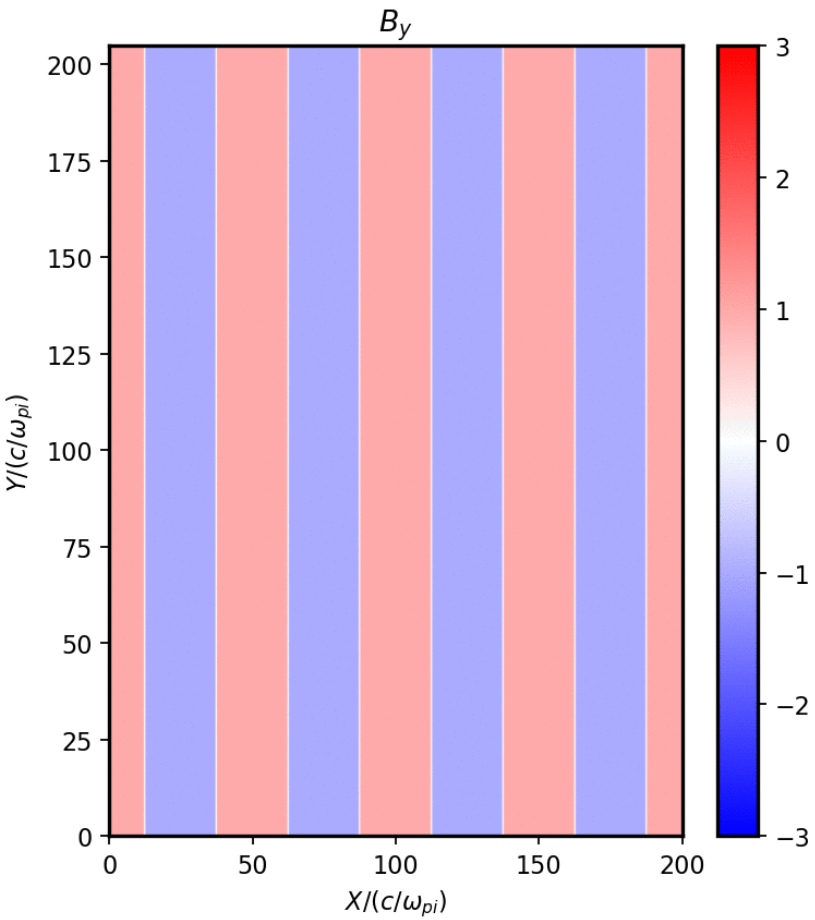

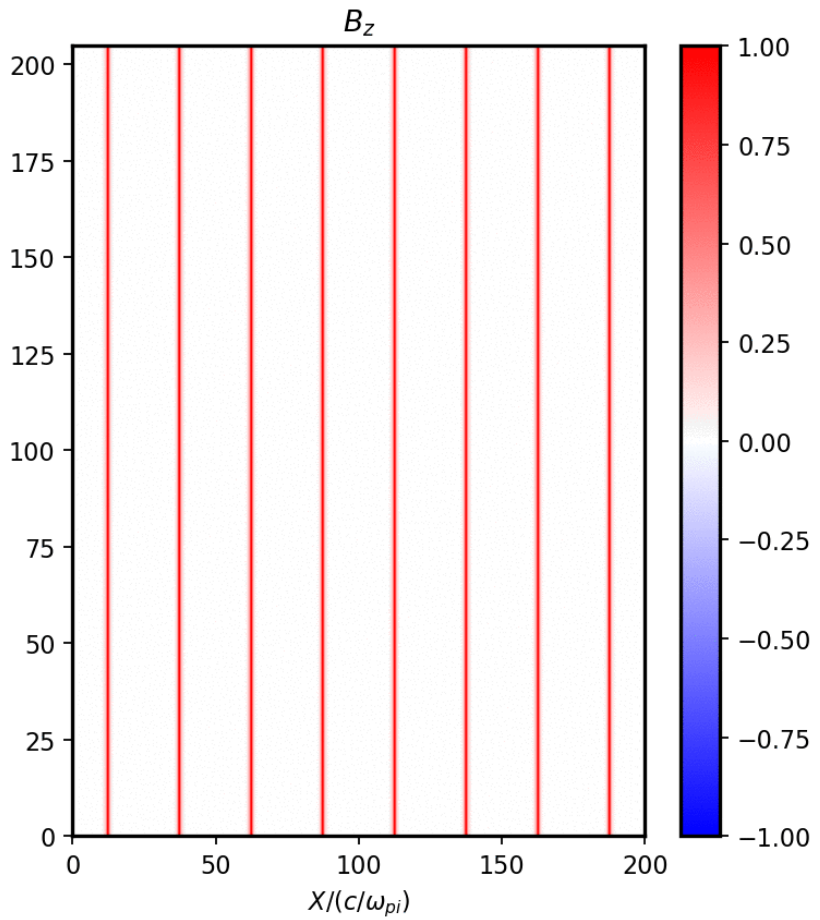

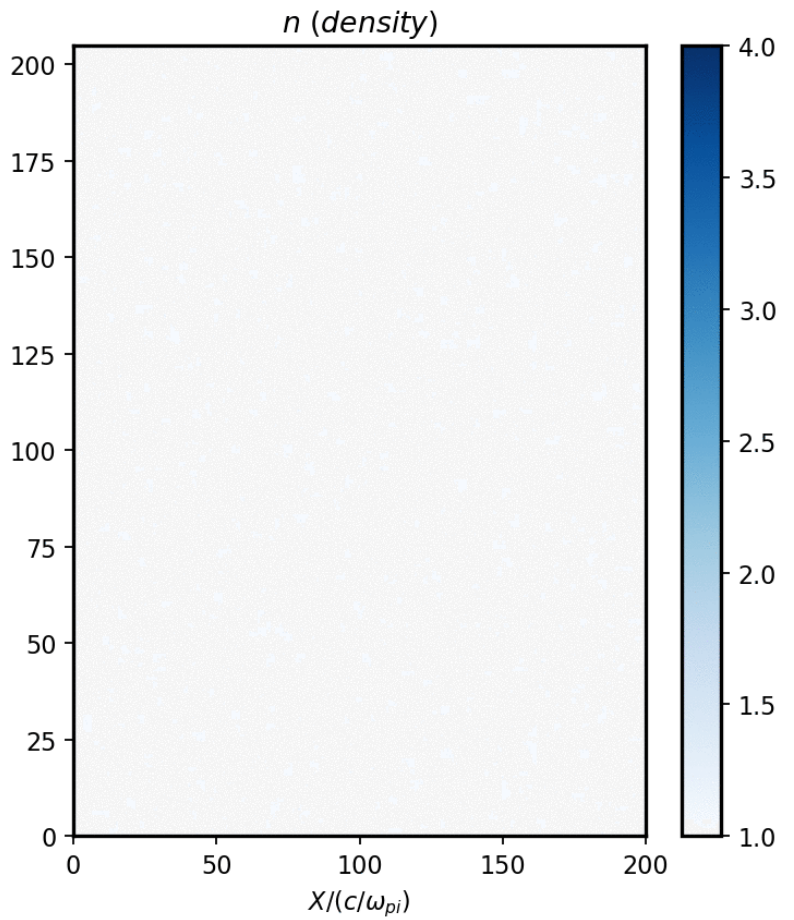

Results: Snapshot of the Interaction of Current Sheets with a Shock Wave

- Current sheets are compressed by the shock wave and become unstable downstream.
- Magnetic fields become turbulent because of reconnection and the merging of islands

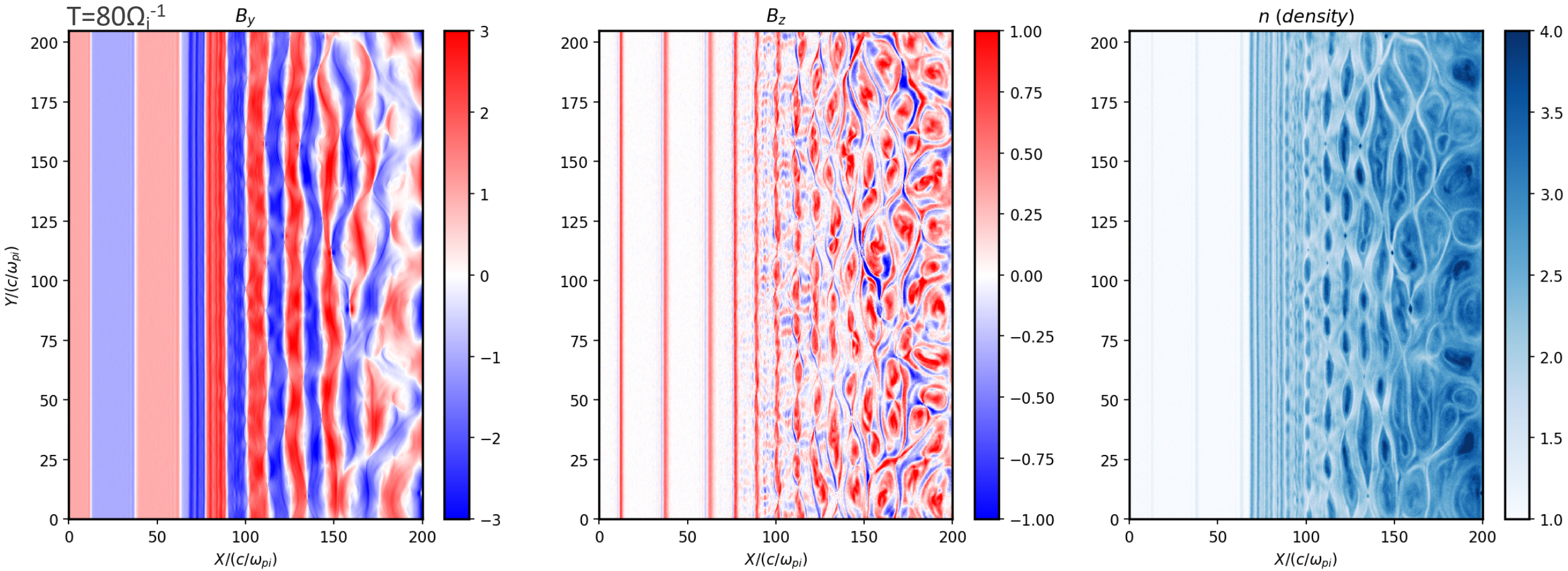

Proton Energy Spectrum:

- Some protons are accelerated at the shock wave (blue line)
- Those accelerated protons are further energized due to reconnection events far downstream
- Black line shows the number of particles satisfying $|v|>5V_A$.
- Flux increases as magnetic reconnection proceeds.

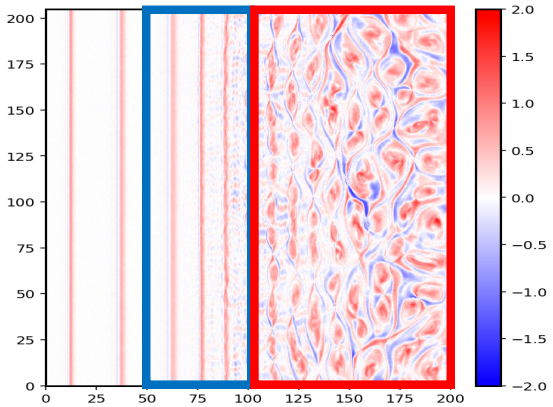

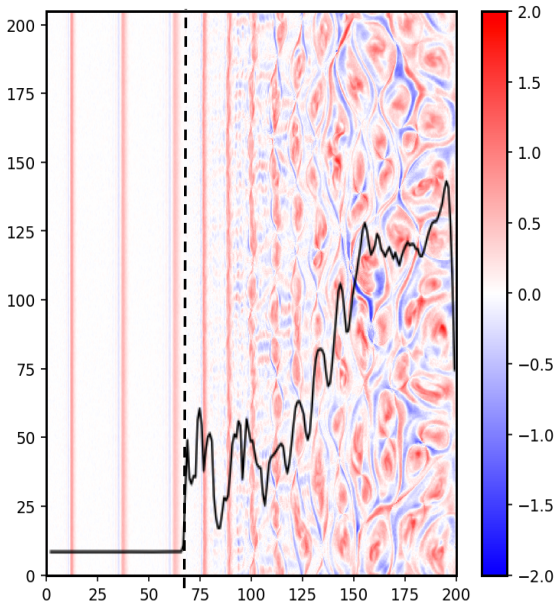

- Flux enhancement responding to magnetic reconnection activity
- Energetic particle profile similar to predicted DSA-reconnection transport model [Zank et al.2015, le Roux et al. 2015].

Nakanotani et al 2020

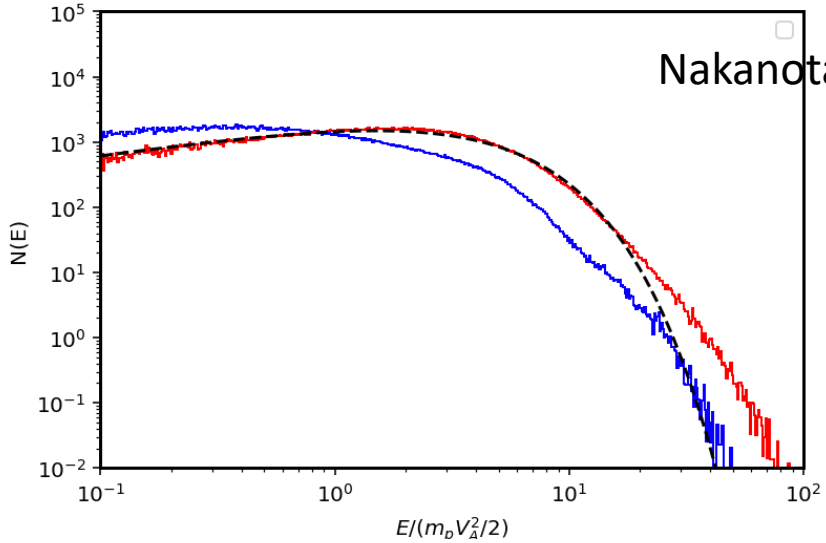

Zhao et al. 2018, 2019a